

Conditions for shock revival by neutrino heating in core-collapse supernovae

H.-Thomas Janka

Max-Planck-Institut für Astrophysik, Karl-Schwarzschild-Straße 1, D-85741 Garching, Germany

December 2, 2024

Abstract. Energy deposition by neutrinos can rejuvenate the stalled bounce shock and can provide the energy for the supernova explosion of a massive star. This neutrino-heating mechanism, though investigated by numerical simulations and analytic studies, is not finally accepted or proven as the trigger of the explosion. Part of the problem is that different groups have obtained seemingly discrepant results, and the complexity of the hydrodynamic models often hampers a clear and simple interpretation of the results. This demands a deeper theoretical understanding of the requirements of a successful shock revival. An approach is described here which allows one to discuss the neutrino heating phase analytically by a time-dependent treatment. This treatment encompasses the cases of accretion as well as mass loss by the nascent neutron star. It is useful to illuminate the conditions that can lead to delayed explosions and in this sense supplements detailed numerical simulations. On grounds of the model developed here, a criterion is derived which formulates the minimum requirements for shock revival. It shows that the success of the supernova shock does not only depend on the neutrino heating in the gain region and the mass infall to the shock. It is also sensitive to the energy loss by neutrino emission in the cooling layer outside the neutrinosphere, which governs the accretion of matter into the nascent neutron star. The analysis shows that neutrino-driven shock expansion and acceleration are neither likely to occur at very early times after core bounce, when the mass infall rate is still very high, nor at late times when the accretion rate has become too low. However, there is a window of conditions, realized at intermediate post-bounce times, where the mass accretion by the shock and the neutrinospheric luminosity define favorable conditions for shock revival. This space of advantageous conditions widens with a larger value of the shock stagnation radius. The importance of convective energy transport in the neutrino-heating region is confirmed, because it reduces the extraction of energy from the gain region

associated with the inward flow of neutrino-heated matter through the gain radius. An enhancement of the neutrinospheric luminosity, besides increasing the neutrino heating, has the helpful effect of diminishing the mass advection into the neutron star.

Key words: supernovae: general – elementary particles: neutrinos – hydrodynamics – accretion

1. Introduction

Neutrinos dominate the energetics of core-collapse supernovae. Only about one percent or $\sim 10^{51}$ erg of the gravitational binding energy released in the formation process of the compact remnant, usually a neutron star, end up as kinetic energy of the expanding ejecta, whereas 99% of this energy are radiated away in neutrinos. Electron captures on protons and nuclei trigger the gravitational instability of the iron core of an evolved massive star, because the electron number and thus the pressure are reduced by the escape of electron neutrinos (see, e.g., Bruenn 1986a). Later the loss of energy by the diffusion of neutrinos and antineutrinos of all flavors drives the evolution of the nascent neutron star from a hot, inflated configuration to the compact and very dense final state (Burrows & Lattimer 1986).

Colgate & White (1966) were the first to suggest that neutrinos may also play a crucial role for the explosion by taking up the gravitational binding energy of the collapsing core and depositing it in the rest of the star. Subsequent improvements and more realistic treatments of the microphysics, like equation of state (EoS) and neutrino transport, have changed our modern picture of stellar core collapse dramatically compared to the pioneering simulations by Colgate & White (1966). Because of the discovery of weak neutral currents and the corresponding importance of neutrino scattering off nucleons and nuclei, the forming neutron star was recognized to be highly

Send offprint requests to: H.-Th. Janka
(thj@mpa-garching.mpg.de)

opaque to neutrinos. Therefore the neutrino luminosities turned out to be too low, and the energy transfer rate by neutrinos not large enough to invert the infall of the surrounding gas into an explosion. For many years, hopes and efforts therefore concentrated on the prompt bounce-shock mechanism: The energy given to the hydrodynamical shock wave in the moment of core bounce was thought to lead directly to the ejection of the stellar mantle and envelope. Detailed models, however, showed that the shock experiences such severe energy losses by photodisintegration of iron nuclei and additional neutrino emission, that its outward propagation stops still well inside the iron core (e.g., Bruenn 1985, 1989a,b, 1993; Hillebrandt 1987; Myra et al. 1987, 1989).

Wilson (1985), however, discovered that neutrinos can indeed cause an explosion on a timescale much longer than previously thought. More than 100 milliseconds after core bounce the conditions for neutrino energy deposition have significantly improved (Bethe & Wilson 1985), and the mass infall rate and thus the ram pressure of the shock have decreased, making an explosion at later times easier than right after bounce (Burrows & Goshy 1993, Bethe 1995). Although Wilson et al. (1986) obtained such “delayed” explosions via the neutrino-heating mechanism, their simulations gave rather low explosion energies, and their successes could not be confirmed by independent models with supposedly superior treatment of the neutrino physics and EoS (Bruenn 1986b, 1989a,b). Later simulations by Wilson & Mayle (1988, 1993) and Mayle & Wilson (1988) included neutron-finger convection in the nascent neutron star, which boosts the neutrino luminosities and thus increases the neutrino heating and the explosion energy. But whether neutron-finger convection actually occurs in the hot neutron star, or Ledoux-type convection (Burrows 1987, Keil et al. 1996, Pons et al. 1999), or none (Bruenn et al. 1995, Mezzacappa et al. 1998a) seems to depend on the properties of the nuclear EoS and possibly also on the treatment of the neutrino physics.

More recently, multi-dimensional simulations showed that convective overturn in the region of net neutrino heating between shock and gain radius (that is the position outside the neutrinosphere where neutrino cooling is balanced by neutrino heating; Bethe & Wilson 1985) can aid the explosion (Herant et al. 1994; Janka & Müller 1995, 1996; Burrows et al. 1995) and can produce successes even when spherically symmetric models fail. This “convective engine” (Herant et al. 1994) or “boiling” (Burrows et al. 1995) transports cool gas into the region of strongest heating while at the same time hot gas rises towards the shock. Both effects increase the efficiency of neutrino energy transfer, reduce the energy loss by the reemission of neutrinos from the heated gas, and raise the postshock pressure, thus leading to more favorable conditions for shock expansion. While the existence and importance of postshock convection is not questioned, simulations with the most advanced treatment of the neutrino

transport applied to multi-dimensional supernova calculations so far (Mezzacappa et al. 1998b, Lichtenstadt et al. 1999) nourished doubts whether the effects of convection are sufficiently strong to cause explosions.

Therefore scepticism about the viability of the delayed explosion mechanism by neutrino heating still remains (Thompson 2000), and seems justified even more because of recent observations which indicate a possible connection between gamma-ray bursts and at least some supernovae (e.g., Galama et al. 1998, Bloom et al. 1999). If confirmed, this discovery would require to consider large energies and/or asphericities of the explosions (Iwamoto et al. 1998, Woosley et al. 1999, Höflich et al. 1999) which might be hard to explain by the neutrino-driven mechanism. Therefore, despite the fact that the observations are still far from being conclusive, theorists feel tempted to speculate about alternative ways to power stellar explosions, e.g., by invoking magnetically driven jets (Wang & Wheeler 1998, Khokhlov et al. 1999). However, while we know about the crucial role of neutrinos, we have no observational evidence or convincing theoretical argument in support of a dynamically important strength of magnetic fields in combination with a significant degree of rotation in the iron cores of all massive stars. Rather than in ordinary core-collapse supernovae, jets and a magnetohydrodynamic mechanism may be at work in cases where the neutrino-driven mechanism definitely fails, e.g., for progenitor main sequence masses above about $25 M_{\odot}$ (Fryer 1999) and when a black hole forms at the center of a rapidly spinning massive star (MacFadyen & Woosley 1999, MacFadyen et al. 1999).

When judging about the viability of the neutrino-driven mechanism, one must, however, keep in mind the enormous complexity of the problem. Because of this complexity a number of approximations and simplifications had to be made in even the currently most refined hydrodynamical calculations. Some of these deficiencies have probably disadvantageous consequences for the efficiency of neutrino energy deposition in the postshock layers. Until very recently, all published hydrodynamical models employed, for example, a still unsatisfactory treatment of the neutrino transport. Instead of solving the Boltzmann transport equation, they used flux-limited diffusion schemes, a fact which underestimates the neutrino heating above the gain radius and overestimates the energy loss by neutrino emission below it (Janka 1991a, 1992; Messer et al. 1998; Yamada et al. 1999). Moreover, multidimensional supernova simulations have so far not been able to resolve the convective processes inside the nascent neutron star, although cooling models of neutron stars show their potential importance (Burrows 1987, Keil et al. 1996, Pons et al. 1999). Even more, recent investigations (e.g., Raffelt & Seckel 1995; Janka et al. 1996; Burrows & Sawyer 1998, 1999; Reddy et al. 1998, 1999; Yamada 2000; Yamada & Toki 2000, and references therein) suggest that neutrino interaction rates in hot nuclear matter are sup-

pressed compared to the standard description used in the numerical codes. Both the latter effects imply that the neutrino luminosities from the post-collapse core are most likely underestimated in current supernova models.

The neutrino-driven mechanism is by its nature sensitive to the neutrino-matter coupling in the heating region, which depends on the properties, i.e., spectra and luminosities, of the neutrino emission from the neutrinosphere and on the angular distribution of the neutrinos exterior to the neutrinosphere (Messer et al. 1998, Yamada et al. 1999, Burrows et al. 2000). These issues require not only the best possible technical treatment of the neutrino transport (cf. Mezzacappa et al. 2000, Liebendörfer et al. 2000, Rampp & Janka 2000) and of the description of the neutrino opacities, but they can vary with the structure of the progenitor star, with general relativity, and with the nuclear EoS and therefore the compactness of the nascent neutron star. Differences of the simulations by different groups may be associated with one or more of these issues. Unfortunately, a detailed analysis and direct comparison is essentially impossible because of largely different numerical approaches and a complicated interdependence of effects.

In this unclear and extremely unsatisfactory situation a better fundamental understanding of the conditions and requirements for shock revival by neutrino heating is highly desirable. Several attempts were made for a discussion by analytic means (Bruenn 1993; Bethe 1993, 1995, 1997; Shigeyama 1995; Thompson 2000) or on grounds of simplified numerical analysis (Burrows & Goshy 1993). While each of them contains interesting aspects and can shed light on certain results of simulations, they have led to contradictory conclusions, and none is general enough to be finally convincing. For example, assuming steady-state conditions (Burrows & Goshy 1993) cannot explain how accretion is reversed into expansion, and why an accretion shock should contract again after moving outward for some while, a possibility which was in fact observed in many hydrodynamical simulations. The beginning of the reexpansion of the stalled shock and the phase when most of the explosion energy is deposited can also not be described by a stationary neutrino-driven baryonic wind (Qian & Woosley 1996). Bethe (1990, 1993, 1995, 1997) gave a very useful and detailed discussion of the physics of neutrino heating, the structure and composition of the heating region, and the shock energetics and nucleosynthesis, using observational constraints from Supernova 1987A and numerical results provided mainly by Jim Wilson. Although addressing the question of the start of the shock, his analysis does not really reveal the requirements for a successful shock revival. Moreover, aspects were disregarded which have been recognized to be important for the outcome of simulations, for example the fact that rapid neutrino losses in the cooling region can weaken or even prevent an explosion (Woosley & Weaver 1994, Janka & Müller 1996, Messer et al. 1998). Bethe arrived at the con-

clusion that the explosion energy is delivered by neutrinos, whereas Bruenn (1993) and Thompson (2000) argued that neutrino heating is insufficient to cause an explosion because the advection timescale of the gas between shock and gain radius is too short for large energy deposition. Shigeyama (1995), on the other hand, performed a quasi-stationary analysis by expanding the physical variables in a power series of a small parameter, but his approach obscures the essential physics of shock revival rather than illuminating them.

The work presented here is a new approach for an analytic discussion of the conditions which can lead to the reexpansion of the supernova shock. The analysis is based on a simplified model for the post-bounce structure of the collapsed stellar core and generalizes the treatment of neutron star accretion by Chevalier (1989; see also Brown & Weingartner 1994, Fryer et al. 1996). It is not meant to yield quantitative results or to be able to compete with detailed hydrodynamical simulations, but it should allow one to reproduce the basic features of the shock stagnation, accretion, and shock revival phases. It is therefore a supplementary tool which helps one getting a qualitative understanding of the processes that determine the post-bounce evolution of the collapsed stellar core. In particular, the relative strength of competing effects that play a role in the neutrino-heating mechanism and their influence on the behavior of the supernova shock, i.e., its radial position and velocity as a function of time, can be estimated. This should help explaining why some models fail to produce explosions while others succeed.

The paper is organized in the following way. In Sect. 2 the physics of the post-bounce accretion phase will be described, in Sect. 3 the basic equations and corresponding assumptions used in the simplified analytic model will be introduced, in Sect. 4 the characteristic radii of the problem and their properties will be formally defined, in Sect. 5 the structure of the collapsed stellar core behind the stalled supernova shock will be discussed, in Sect. 6 expressions for the neutrino heating and cooling will be derived, in Sect. 7 the mass accretion rate of the nascent neutron star will be calculated, and in Sect. 8 the equations of mass and energy conservation will be applied to the neutrino heating layer, which leads to relations which are crucial for determining the radius and the velocity of the supernova shock. From these relations a criterion for the revival of a stalled supernova shock will be deduced in Sect. 9. The formalism developed in this paper will then be used to discuss the conditions for delayed explosions. A summary and conclusions will follow in Sect. 10.

2. Physical picture

Right after core bounce the hydrodynamic shock propagates outward in mass as well as in radius, being strongly damped by energy losses due to the photodisintegration of iron-group nuclei and neutrinos. The neutrino emis-

sion rises significantly when the shock breaks out into the neutrino-transparent regime. As a consequence, the pressure behind the shock is reduced and the velocities of the shock and of the fluid behind the shock, both of which were positive initially, decrease. Finally, the outward expansion of the shock stagnates, and the shock transforms into a standing accretion shock with negative gas velocity in the postshock region. The gas of the progenitor star, which continues to fall into the shock at a velocity near free fall, is decelerated abruptly within the shock. Below the shock it moves much more slowly towards the center, where it settles onto the surface of the nascent neutron star.

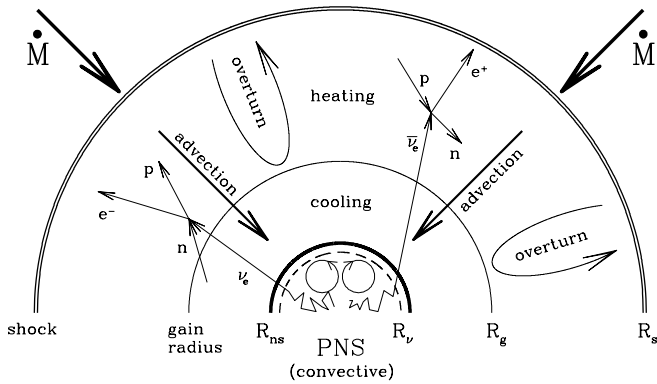


Fig. 1. Sketch which summarizes the processes that determine the evolution of the stalled supernova shock after core bounce. Stellar matter falls into the shock at radius R_s with a mass accretion rate \dot{M} and a velocity near free fall. After deceleration in the shock, the gas is much more slowly advected towards the nascent neutron star through the regions of net neutrino heating and cooling, respectively. The radius R_{ns} of the neutron star is defined by a steep decline of the density over several orders of magnitude outside the neutrinosphere at R_ν . Heating balances cooling at the gain radius R_g . The dominant processes of energy deposition and loss are absorption of electron neutrinos onto neutrons and electron antineutrinos onto protons as indicated in the figure. Convective overturn mixes the layer between gain radius and shock, and convection inside the neutron star helps the explosion by boosting the neutrino luminosities.

Figure 1 displays the most important physical elements which determine this evolutionary stage. Around the neutrinosphere at radius R_ν , which is close to the radius R_{ns} of the proto-neutron star (PNS), the hot and comparatively dense gas loses energy by radiating neutrinos. If this energy sink were absent, the gas that is accreted through the shock at a rate \dot{M} would pile up in a growing, high-entropy atmosphere on top of the compact remnant (Colgate et al. 1993, Colgate & Fryer 1995, Fryer et al. 1996). But since neutrinos are emitted efficiently at the thermodynamical conditions around the neutrinosphere, the entropy of the gas is reduced so that

the gas can be absorbed into the surface of the neutron star. The mass flow through the neutrinospheric region is therefore triggered by the neutrino energy loss and allows more gas to be advected inward from larger radii. In case of stationary accretion the temperature at the base of the atmosphere ensures that the emitted neutrinos carry away the gravitational binding energy of the matter which is added to the neutron star at a given accretion rate. In fact, this requirement closes the set of equations that determines the steady state of the accretion system and allows one to determine the radius R_s of the accretion shock (see, e.g., Chevalier 1989, Brown & Weingartner 1994, Fryer et al. 1996).

At the so-called gain radius R_g (Bethe & Wilson 1985) between neutrinosphere R_ν and shock position R_s , the temperature of the atmosphere becomes so low that the absorption of high-energy electron neutrinos and antineutrinos starts to exceed the neutrino emission. This radius therefore separates the region of net neutrino cooling below from a layer of net heating above. Since the neutrino heating is strongest just outside the gain radius and the propagation of the shock has weakened before stagnation, a negative entropy gradient is built up in the postshock region. This leads to convective overturn roughly between R_g and R_s , which transports hot matter outward in rising high-entropy bubbles. At the same time cooler material is mixed inward in narrow, low-entropy downflows (Herant et al. 1994, Burrows et al. 1995, Janka & Müller 1996). Inside the nascent neutron star, below the neutrinosphere, convective motions can enhance the neutrino emission by carrying energy faster to the surface than neutrino diffusion does (Keil et al. 1996).

Between neutrinosphere and the supernova shock a number of approximations apply to a high degree of accuracy, which help one developing a simple analytic understanding of the effects that influence the evolution of the supernova shock. Figure 2 shows schematically the profiles of density, temperature and mass accretion rate in that region. A formal discussion follows in the subsequent sections. Outside the neutrinosphere (typically at about 10^{11} g/cm³) the temperature drops slowly compared to the density decline, which is steep. When nonrelativistic nucleons dominate the pressure, the decrease of the density yields the pressure gradient which ensures hydrostatic equilibrium in the gravitational field of the neutron star. Assuming a temperature equal to the neutrinospheric temperature in this region is a reasonably good approximation for the following reasons. On the one hand, the cooling rate depends sensitively both on density and temperature, and the density drops rapidly. Therefore the total energy loss is determined in the immediate vicinity of the neutrinosphere and the details of the temperature profile do not matter very much. On the other hand, efficient neutrino heating prevents that the temperature can drop much below the neutrinospheric value. If, instead, the temperature would rise significantly above this latter value, the matter

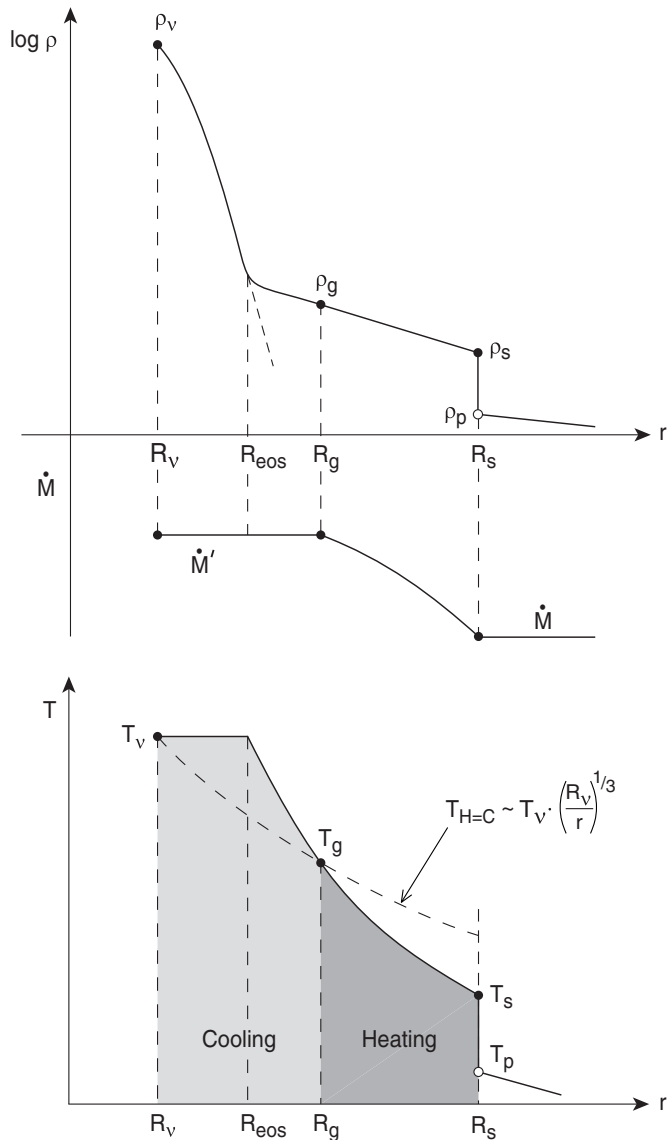


Fig. 2. Schematic profiles of density, temperature, and mass accretion rate between neutrinosphere at radius R_ν and shock at R_s some time after core bounce. R_g denotes the position of the gain radius. At the shock, ρ and T jump discontinuously from their preshock values ρ_p and T_p to the postshock values ρ_s and T_s , respectively. For $r < R_{eos}$ the density declines steeply because the pressure is mainly caused by the nonrelativistic Boltzmann gases of free neutrons and protons. Outside of R_{eos} the gas is radiation dominated and the density decrease much flatter. In general, some of the gas falling into the shock at rate \dot{M} may stay in the region of neutrino heating while another part (rate \dot{M}') is advected into the nascent neutron star. Note that $\dot{M}(r)$ is continuous at the shock in the rest frame of the star only in case of a stalled shock front. Between R_ν and R_{eos} the temperature can be considered roughly as constant, whereas its negative gradient in the radiation dominated region ensures hydrostatic equilibrium. There is net energy loss between R_ν and R_g where $T(r)$ exceeds the temperature $T_{H=C} \sim T_\nu (R_\nu/r)^{1/3}$, for which neutrino heating equals cooling. Net energy deposition occurs between R_g and R_s .

would become optically thick to the energetic neutrinos produced in the hot gas (the opacity increases roughly with the square of the neutrino energy) and the neutrinosphere would move farther out to a lower density (and thus typically a lower temperature).

Below a density between 10^9 g/cm^3 and 10^{10} g/cm^3 , relativistic electron-positron pairs and radiation determine the pressure, provided the temperature is sufficiently high, typically around 1 MeV or more (see Woosley et al. 1986). Exterior to the corresponding radius R_{eos} , where this transition from the baryon-dominated to the radiation-dominated regime takes place, the temperature must therefore decrease so that the negative temperature gradient can yield the force which balances gravity.

The gain radius R_g is located at the radial position where the temperature profile $T(r)$ intersects with the curve of temperature values, $T_{H=C}(r)$, for which heating is equal to cooling by neutrinos, roughly given by

$$T_{H=C}(r) \sim T_\nu \cdot \left(\frac{R_\nu}{r}\right)^{1/3} \quad (1)$$

(Bethe & Wilson 1985). In Eq. (1) T_ν means the temperature at the radius R_ν of the neutrinosphere. The shock at R_s is taken to be infinitesimally thin compared to the scales considered. Within the shock the density and temperature therefore jump from their preshock values ρ_p and T_p , to the postshock values ρ_s and T_s , respectively. A part of the gas which falls into the shock with a mass accretion rate \dot{M} can stay in the region of neutrino heating, whereas another part is advected with rate \dot{M}' through the cooling region to be added to the neutron star inside R_ν .

In this paper the discussion will be restricted to an idealized, spherically symmetric situation and possible convective mixing will be assumed to lead to efficient homogenization of the unstable layer. Certainly, this is not a good assumption for the convective overturn that takes place in the region between gain radius and shock front, where prominent, large-scale inhomogeneities develop (Herant et al. 1994, Burrows et al. 1995, Janka & Müller 1996). Bethe (1995) has made attempts to discuss the physical implications of the simultaneous presence of low-entropy downstreams and high-entropy rising bubbles. For this purpose he introduced free parameters, e.g., to quantify the fraction of neutrinos that hits the cold downflows and is effective for their heating, or to account for the part of the matter that is added to the neutron star instead of being pushed outward in the expanding bubbles. This procedure is not really satisfactory and will not be copied here. Instead, an admittedly simplified and idealized spherical situation will be considered to highlight the conditions needed for shock revival and to develop a qualitative understanding of the influence of different effects. One-dimensional analysis can help developing a better understanding of the delayed explosion mechanism, because simulations in spherical symmetry have produced successful explosions (Wilson 1985; Wilson et al. 1986; Janka &

Müller 1995, 1996; Mezzacappa et al. 2000). Thus they have demonstrated that convection behind the shock is not an indispensable requirement for an explosion, although it may be an essential (Herant et al. 1994, Burrows et al. 1995, Janka & Müller 1996) — yet not necessarily sufficient (Janka & Müller 1996, Mezzacappa et al. 1998b, Lichtenstadt et al. 1999) — ingredient to obtain explosions, or to raise the explosion energy in cases which fail or nearly fail in spherical symmetry.

3. Basic equations and assumptions

The hydrodynamic equations are considered in Eulerian form for spherical symmetry with source terms for Newtonian gravity and neutrino energy and momentum exchange with the stellar medium. The equations of continuity, momentum, and energy are:

$$\frac{\partial \rho}{\partial t} + \frac{1}{r^2} \frac{\partial}{\partial r} (r^2 \rho v) = 0, \quad (2)$$

$$\frac{\partial(\rho v)}{\partial t} + \frac{1}{r^2} \frac{\partial}{\partial r} (r^2 \rho v^2) = -\frac{\partial P}{\partial r} - \rho \frac{\partial \Phi}{\partial r}, \quad (3)$$

$$\frac{\partial e}{\partial t} + \frac{1}{r^2} \frac{\partial}{\partial r} [r^2 v (e + P)] = -\rho v \frac{\partial \Phi}{\partial r} + Q_\nu. \quad (4)$$

Here r , v , ρ , P , t are radius, fluid velocity, density, pressure, and time, respectively, and e is defined as the sum of internal energy density, ε , and kinetic energy density of the gas:

$$e = \frac{1}{2} \rho v^2 + \varepsilon. \quad (5)$$

The term Q_ν denotes the rate of energy gain or loss per unit volume by neutrino heating and cooling. $\Phi(r)$ is an effective potential which contains contributions from the gravitational potential and from the momentum transfer to the stellar gas by neutrinos. Neglecting self-gravity of the gas in the region between neutrinosphere and supernova shock, it can be written as

$$\Phi = -\frac{G\widetilde{M}}{r} = -\frac{G}{r} \left(M - \frac{\langle \kappa_t \rangle L_\nu}{4\pi G c \rho} \right). \quad (6)$$

Here G is the gravitational constant, c the speed of light, M the mass inside R_ν and \widetilde{M} means an effective mass that includes the momentum transfer term and is defined by the term in brackets on the right side of Eq. (6). When self-gravity is disregarded, the mass of the gas between R_ν and R_s must be negligible compared to the neutron star mass M , i.e.,

$$\Delta M = \int_{R_\nu}^{R_s} dr 4\pi r^2 \rho(r) \ll M. \quad (7)$$

In Eq. (6) $L_\nu = \sum_{\nu_i} L_{\nu_i}$ is the total neutrino luminosity and $\langle \kappa_t \rangle$ the mean total opacity calculated as an

average of the total opacities of neutrinos ν_i and antineutrinos $\bar{\nu}_i$ of all flavors according to

$$\langle \kappa_t \rangle L_\nu \equiv \sum_{\nu_i} \kappa_{t,\nu_i} L_{\nu_i} + \sum_{\bar{\nu}_i} \kappa_{t,\bar{\nu}_i} L_{\bar{\nu}_i}. \quad (8)$$

Note that the total opacity κ_{t,ν_i} of neutrino ν_i is averaged over the spectrum of the corresponding energy flux. Equations (3), (4), and (6) imply that the momentum transfer rate from neutrinos to the stellar gas is written as $\langle \kappa_t \rangle L_\nu / (4\pi c r^2)$ with L_ν and $\langle \kappa_t \rangle / \rho$ not depending on r . This is approximately fulfilled in the optically thin regime for neutrinos, i.e., exterior to the neutrinosphere where the neutrino luminosities and spectra are roughly constant. Yet it is not exactly true, because the concept of “the” neutrinosphere is fuzzy and neutrino emission and absorption continue even outside the neutrinosphere. In addition, the opacity depends on the composition which varies with the radius. During all of the post-bounce evolution, however, the typical total neutrino luminosity is only a few per cent of the Eddington luminosity,

$$L_{\text{Edd},\nu} \equiv \frac{4\pi G M c \rho}{\langle \kappa_t \rangle}. \quad (9)$$

Therefore the neutrino source terms for momentum in Eq. (3) and for kinetic energy in Eq. (4), which are carried by the potential Φ , are always small and the approximate treatment following below is justified.

Neutrinos transfer momentum to the stellar medium by neutral-current scatterings off neutrons and protons. The corresponding transport opacity for these scattering processes is

$$\kappa_{\text{sc}} \approx \frac{5\alpha^2 + 1}{24} \frac{\sigma_0 \langle \epsilon_\nu^2 \rangle}{(m_e c^2)^2} \frac{\rho}{m_u} (Y_n + Y_p). \quad (10)$$

Here $m_u \approx 1.66 \times 10^{-24}$ g is the atomic mass unit, $m_e c^2 = 0.511$ MeV the rest-mass energy of the electron, $\sigma_0 = 1.76 \times 10^{-44}$ cm², and $Y_n = n_n/n_b$ and $Y_p = n_p/n_b$ are the number fractions of free neutrons and protons, i.e., their particle densities normalized to the number density n_b of nucleons. A minor difference between the neutrino-proton and the neutrino-neutron scattering cross section due to different vector coupling constants is ignored, and also the axial-vector couplings are assumed to be the same and to be equal to the charged-current axial-vector coupling constant in vacuum, $\alpha = 1.26$. Additional scattering reactions with electrons and positrons can be neglected because of their much smaller cross sections, and neutrino scattering off nuclei is unimportant because the post-bounce medium exterior to the neutrinosphere is nearly completely disintegrated into free nucleons.

In case of ν_e and $\bar{\nu}_e$ also the charged-current absorptions on neutrons and protons, respectively, need to be taken into account due to their large cross sections. The absorption opacity is

$$\kappa_{\text{a}} \approx \frac{3\alpha^2 + 1}{4} \frac{\sigma_0 \langle \epsilon_\nu^2 \rangle}{(m_e c^2)^2} \frac{\rho}{m_u} \left\{ \begin{array}{l} Y_n \\ Y_p \end{array} \right\}. \quad (11)$$

In Eqs. (10) and (11) the recoil of the nucleon and phase space blocking effects for the fermions are neglected, which is very good at the conditions considered in this paper. In both neutral-current and charged-current processes only the leading terms depending on the squared neutrino energy, ϵ_ν^2 , are taken into account. Averaging over the spectrum of the neutrino energy flux yields the factor $\langle \epsilon_\nu^2 \rangle$, for which Eq. (25) provides a suitable definition, if minor differences between the spectra of neutrino energy density and flux density are disregarded.

Note that the opacities κ_{sc} and κ_{a} are inverse mean free paths and thus measured in units of 1/cm. The total opacity includes the contributions from scattering and absorption and is given as $\kappa_{\text{t},\nu_i} = \kappa_{\text{sc},\nu_i} + \kappa_{\text{a},\nu_i}$. With typical values $L_{\nu_e} = L_{\bar{\nu}_e} = L_{\nu_x} = \frac{1}{6}L_\nu$ (with $\nu_x \in \{\nu_\mu, \bar{\nu}_\mu, \nu_\tau, \bar{\nu}_\tau\}$) and L_{ν_x} being the luminosity of each individual type of ν_x , $\langle \epsilon_{\bar{\nu}_e}^2 \rangle \approx 2\langle \epsilon_{\nu_e}^2 \rangle$ and $\langle \epsilon_{\nu_x}^2 \rangle \approx 4\langle \epsilon_{\nu_e}^2 \rangle$, the total opacity averaged for all neutrinos and antineutrinos can be estimated from Eq. (8) as

$$\begin{aligned} \langle \kappa_{\text{t}} \rangle &\approx \frac{113\alpha^2 + 25}{144} \frac{\sigma_0 \langle \epsilon_{\nu_e}^2 \rangle}{(m_e c^2)^2} \frac{\rho}{m_{\text{u}}} (Y_n + Y_p) \\ &\approx 1.9 \times 10^{-7} \rho_{10} \left(\frac{kT_{\nu_e}}{4 \text{ MeV}} \right)^2 \left[\frac{1}{\text{cm}} \right]. \end{aligned} \quad (12)$$

Since $Y_p < Y_n$ between the neutrinosphere and the shock, $Y_n + 2Y_p \approx Y_n + Y_p$ is a reasonably good approximation in the absorption term. In the second equation use was made of $Y_n + Y_p \approx 1$. If the neutrino flux spectrum has Fermi-Dirac shape with vanishing degeneracy, the neutrino temperature T_ν is related to the mean squared neutrino energy by $\langle \epsilon_\nu^2 \rangle \approx 21 (kT_\nu)^2$. k is the Boltzmann constant and ρ_{10} the density measured in 10^{10} g/cm^3 . For a total neutrino luminosity $L_\nu = 10^{53} \text{ erg/s}$, neutrino momentum transfer reduces \dot{M} in Eq. (6) relative to M by about $3.8 \times 10^{-2} M_\odot$, which is indeed a small correction.

4. The characteristic radii

The neutrinospheric radius R_ν , the gain radius R_g and the transition radius of the EoS properties, R_{eos} , will be formally defined below. They are characteristic of the atmospheric structure in the postshock region, which determines, together with the infall region ahead of the shock, the shock radius R_s and the shock velocity $U_s \equiv \dot{R}_s$.

4.1. The neutrinosphere

The neutrinosphere relevant for the discussion in the following sections is the “energy-sphere”, where neutrinos decouple energetically from the stellar background. It usually does not coincide with the sphere of last scattering, the so-called “transport-sphere”, outside of which the neutrino distribution becomes strongly forward peaked (for a detailed discussion, see Janka 1995). Only inside their energy-sphere neutrinos can be considered to be roughly

in thermodynamic equilibrium with the stellar medium. Besides neutrino-nucleon scattering, which is important for all neutrinos, electron neutrinos ν_e and electron antineutrinos $\bar{\nu}_e$ interact via frequent charged-current absorption and emission reactions with nucleons, whereas muon and tau neutrinos and antineutrinos do not. Therefore the energy-spheres of electron neutrinos and antineutrinos are typically located farther out in the star at larger radii than those of muon and tau neutrinos.

The energy deposition in the gain region, however, is clearly dominated by ν_e and $\bar{\nu}_e$. For this reason one can concentrate on their transport properties and neglect muon and tau neutrinos and antineutrinos in the discussion. Scattering off nucleons acts on all neutrinos equally. The charged-current absorption reactions of ν_e and $\bar{\nu}_e$ on neutrons and protons, respectively, yield an even larger contribution to the total opacity. The opacities of ν_e and $\bar{\nu}_e$ are nearly equal, because $\bar{\nu}_e$ absorption and emission [Eq. (18)] is similarly frequent as ν_e absorption and emission [Eq. (17)] as long as positrons are abundant, i.e., the stellar atmosphere is hot and electrons are not very degenerate. Therefore the transport-spheres and energy-spheres of electron neutrinos and antineutrinos are all close together and it is justified to consider only one, “the”, neutrinosphere at radius R_ν . Of course, the real situation is more complex and there is no definite radius interior to which neutrinos are in equilibrium at the local thermodynamical conditions and diffuse, and exterior to which they are decoupled from the background and stream freely. The transition between these two limits is continuous and in case of neutrinos, whose reaction rates are strongly energy dependent, it is also a function of the neutrino energy.

The spectral temperature of electron neutrinos will be taken equal to the gas temperature at the assumed neutrinosphere, $kT_{\nu_e} = kT(R_\nu)$. Detailed simulations of neutrino transport show that electron antineutrinos have somewhat more energetic spectra. A typical result (e.g., Bruenn 1993, Janka 1991a) is $kT_{\bar{\nu}_e} \approx 1.5 kT_{\nu_e}$, which will be used below. The fact that ν_e and $\bar{\nu}_e$ spectra are found to be different in detailed models is an indication that the picture drawn above is overly simplified. Nevertheless it is sufficiently accurate for the analysis in this paper. Note that in general the neutrino luminosity L_ν can not be related to the neutrinospheric temperature by the Stefan-Boltzmann law for blackbody emission of a sphere with radius R_ν , $L_\nu = \pi R_\nu^2 \frac{7}{8} a c (kT_\nu)^4$. This formula is frequently taken for the combined luminosity of neutrinos plus antineutrinos, assuming their chemical potentials to be zero. However, the effective temperature kT_{eff} , which should be used in the Stefan-Boltzmann law, is typically not equal to the spectral temperature kT_ν (for a discussion, see Janka 1995). Transport simulations show that due to non-equilibrium effects the difference can be quite significant. For this reason two parameters, T_ν and L_ν , will be retained here to describe the spectrum and the luminosity of the neutrinos emitted from the neutrinosphere.

Moreover, the radius of the neutrinosphere will be considered as the position in the star where the mean value of the cosine of the neutrino propagation angle relative to the radial direction has a value of 0.25 [see Eq. (26) and Janka 1991a,b, 1995].

Keeping in mind the simplifications associated with the concept of the neutrinosphere, the radius R_ν can be defined by the requirement that the effective optical depth to energy exchange for neutrinos with average energy is

$$\tau_{\text{eff}} = \int_{R_\nu}^{\infty} dr \kappa_{\text{eff}}(r) = \frac{2}{3} \quad (13)$$

(Suzuki 1989). The effective opacity κ_{eff} in case of ν_e and $\bar{\nu}_e$ is defined from the scattering opacity κ_{sc} and the absorption opacity κ_a as

$$\kappa_{\text{eff}} = \sqrt{\kappa_a (\kappa_a + \kappa_{\text{sc}})} \quad (14)$$

(Rybicki & Lightman 1979, Shapiro & Teukolsky 1983, Suzuki 1989). Using Eqs. (10) and (11) one obtains for the effective opacity, again averaged over the spectrum of the energy flux which is supposed to have Fermi-Dirac shape with zero degeneracy, in case of electron neutrinos the expression

$$\begin{aligned} \kappa_{\text{eff},\nu_e} &= 1.62 \frac{\sigma_0 \langle \epsilon_{\nu_e}^2 \rangle}{(m_e c^2)^2} \frac{\rho}{m_u} Y_n \sqrt{1 + 0.21 \frac{Y_p}{Y_n}} \\ &= 2.2 \times 10^{-7} \rho_{10} \left(\frac{kT_{\nu_e}}{4 \text{ MeV}} \right)^2 Y_n \sqrt{1 + 0.21 \frac{Y_p}{Y_n}}, \end{aligned} \quad (15)$$

and in case of electron antineutrinos the analogue result with $Y_n \sqrt{1 + 0.21 Y_p/Y_n}$ being replaced by $Y_p \sqrt{1 + 0.21 Y_n/Y_p}$. Since nuclei are nearly completely dissociated into free nucleons and Y_n is larger than Y_p , i.e., $Y_n \sim 0.8$ and $Y_p \sim 0.2$, but kT_{ν_e} is usually somewhat lower than $kT_{\bar{\nu}_e}$, i.e., $kT_{\nu_e} \approx 4 \text{ MeV}$ and $kT_{\bar{\nu}_e} \approx 6 \text{ MeV}$, we verify the above statement that the effective opacities of ν_e and $\bar{\nu}_e$ are approximately equal. Assuming equal luminosities, $L_{\nu_e} = L_{\bar{\nu}_e}$, a suitable average value for the effective opacity therefore is

$$\begin{aligned} \langle \kappa_{\text{eff}} \rangle &= \frac{1}{2} \kappa_{\text{eff},\nu_e} + \frac{1}{2} \kappa_{\text{eff},\bar{\nu}_e} \\ &\approx 1.5 \times 10^{-7} \rho_{10} \left(\frac{kT_{\nu_e}}{4 \text{ MeV}} \right)^2, \end{aligned} \quad (16)$$

where the composition dependent term in the weighted average has been approximated by $\sqrt{2}$. Knowing the density profile $\rho(r)$, the density ρ_ν at the neutrinosphere can be determined by using Eq. (16) in Eq. (13).

4.2. The gain radius

Heating and cooling of the gas outside the neutrinosphere mainly proceed via the charged-current absorption and

emission processes of ν_e and $\bar{\nu}_e$ (Bethe & Wilson 1985; Bethe 1993, 1995, 1997):

$$\nu_e + n \longleftrightarrow p + e^-, \quad (17)$$

$$\bar{\nu}_e + p \longleftrightarrow n + e^+. \quad (18)$$

To leading order in the particle energies, the cross sections for neutrino and electron/positron absorption, respectively, are

$$\sigma_{a,\nu_e} \approx \sigma_{a,\bar{\nu}_e} \approx \frac{3\alpha^2 + 1}{4} \sigma_0 \left(\frac{\epsilon_\nu}{m_e c^2} \right)^2, \quad (19)$$

$$\sigma_{a,e^-} \approx \sigma_{a,e^+} \approx \frac{3\alpha^2 + 1}{8} \sigma_0 \left(\frac{\epsilon_e}{m_e c^2} \right)^2. \quad (20)$$

At the considered densities and temperatures, fermion phase space blocking and dense-medium effects can be safely ignored, and electrons are relativistic ($kT \gtrsim m_e c^2$). The heating rate $Q_{\nu_i}^+$ of the stellar medium by neutrinos ν_i is given by

$$Q_{\nu_i}^+ = \frac{3\alpha^2 + 1}{4} \frac{\sigma_0 c n_j}{(m_e c^2)^2} \int_0^\infty d\epsilon_\nu \int_{-1}^{+1} d\mu \frac{d^2 n_{\nu_i}}{d\epsilon_\nu d\mu} \epsilon_\nu^3, \quad (21)$$

where n_j is the number density of the target nucleons ($j = p, n$), and $d^2 n_{\nu_i}/(d\epsilon_\nu d\mu)$ the neutrino distribution,

$$\frac{d^2 n_{\nu_i}}{d\epsilon_\nu d\mu} = \frac{2\pi}{(hc)^3} f_{\nu_i}(\epsilon_\nu, \mu) \epsilon_\nu^2, \quad (22)$$

with $f_{\nu_i}(\epsilon_\nu, \mu)$ being the neutrino phase space occupation function at some radius r , which depends on the neutrino energy ϵ_ν and the cosine of the angle of neutrino propagation relative to the radial direction, $\mu = \cos \theta$. In Eq. (22) the factor h in the denominator is Planck's constant. Introducing Eq. (22) into Eq. (21) and performing the phase space integration over all energies and angles yields

$$Q_{\nu_i}^+ = \frac{3\alpha^2 + 1}{4} \sigma_0 n_j \frac{\langle \epsilon_{\nu_i}^2 \rangle}{(m_e c^2)^2} \frac{L_{\nu_i}}{4\pi r^2 \langle \mu_{\nu_i} \rangle}. \quad (23)$$

Here the neutrino luminosity L_{ν_i} , the average squared neutrino energy $\langle \epsilon_{\nu_i}^2 \rangle$, and the mean value of the cosine of the propagation angle, $\langle \mu_{\nu_i} \rangle$, are calculated from the neutrino phase space occupation function $f_{\nu_i}(\epsilon_\nu, \mu)$ by

$$L_{\nu_i} = 4\pi r^2 c \frac{2\pi}{(hc)^3} \int_0^\infty d\epsilon_\nu \int_{-1}^{+1} d\mu \mu \epsilon_\nu^3 f_{\nu_i}(\epsilon_\nu, \mu), \quad (24)$$

$$\langle \epsilon_{\nu_i}^2 \rangle = \int_0^\infty d\epsilon_\nu \int_{-1}^{+1} d\mu \epsilon_\nu^5 f_{\nu_i} \left(\int_0^\infty d\epsilon_\nu \int_{-1}^{+1} d\mu \epsilon_\nu^3 f_{\nu_i} \right)^{-1}, \quad (25)$$

$$\langle \mu_{\nu_i} \rangle = \int_0^\infty d\epsilon_\nu \int_{-1}^{+1} d\mu \mu \epsilon_\nu^3 f_{\nu_i} \left(\int_0^\infty d\epsilon_\nu \int_{-1}^{+1} d\mu \epsilon_\nu^3 f_{\nu_i} \right)^{-1}. \quad (26)$$

The quantity $\langle\mu_\nu\rangle$ is also called flux factor and can be understood as the ratio of the neutrino energy flux, $L_\nu/(4\pi r^2)$, to the neutrino energy density times c . Typically, it is close to 0.25 near the neutrinosphere of ν_e and $\bar{\nu}_e$ and approaches unity when the neutrino distribution get more and more forward peaked in the limit of free streaming with increasing distance from the neutrinosphere (Janka 1991b, 1992, 1995). The total heating rate Q_ν^+ is the sum of the contributions from ν_e and $\bar{\nu}_e$:

$$Q_\nu^+ = Q_{\nu_e}^+ + Q_{\bar{\nu}_e}^+. \quad (27)$$

To derive a simple expression, one can again assume that $L_{\nu_e} \approx L_{\bar{\nu}_e}$, $\langle\epsilon_{\nu_e}^2\rangle \approx 2\langle\epsilon_{\bar{\nu}_e}^2\rangle$, and that the ν_e spectrum has Fermi-Dirac shape with zero degeneracy, i.e., $\langle\epsilon_{\nu_e}^2\rangle \approx 21(kT_{\nu_e})^2$. In addition, the equality $\langle\mu_{\nu_e}\rangle = \langle\mu_{\bar{\nu}_e}\rangle \equiv \langle\mu_\nu\rangle$ is reasonably well fulfilled because the opacities of electron neutrinos and antineutrinos are very similar and therefore the neutrinospheres of both of them are nearly at the same radius. Putting everything together, the heating rate per unit volume is derived as

$$Q_\nu^+ = \frac{3\alpha^2 + 1}{4} \frac{\sigma_0 \langle\epsilon_{\nu_e}^2\rangle}{(m_e c^2)^2} \frac{\rho}{m_u} \frac{L_{\nu_e}}{4\pi r^2 \langle\mu_\nu\rangle} (Y_n + 2Y_p) \\ \approx 160 \frac{\rho}{m_u} \frac{L_{\nu_e,52}}{r_7^2 \langle\mu_\nu\rangle} \left(\frac{kT_{\nu_e}}{4 \text{ MeV}}\right)^2 \left[\frac{\text{MeV}}{\text{s}}\right]. \quad (28)$$

The numerical factor gives the rate in MeV per baryon, r_7 is the radius in 10^7 cm, and $L_{\nu_e,52}$ the ν_e luminosity normalized to 10^{52} erg/s. In the layers where most of the heating and cooling between neutrinosphere and shock take place, nuclei are nearly fully dissociated into free nucleons (Bethe 1993, 1995, 1997; Thompson 2000) and $Y_p < Y_n$, therefore using $Y_n + 2Y_p \approx 1$ in the last expression is a reasonable approximation.

The cooling rate of the stellar gas by emission of ν_e and $\bar{\nu}_e$ is calculated as

$$Q_\nu^- = \frac{3\alpha^2 + 1}{8} \frac{\sigma_0 c}{(m_e c^2)^2} \int_0^\infty d\epsilon \epsilon^3 \left(n_p \frac{dn_{e^-}}{d\epsilon} + n_n \frac{dn_{e^+}}{d\epsilon} \right), \quad (29)$$

where use was made of Eq. (20), and the distributions of relativistic electrons and positrons are given by

$$\frac{dn_{e^\pm}}{d\epsilon} = \frac{8\pi}{(hc)^3} \frac{\epsilon^2}{1 + \exp(\epsilon/kT - \eta_{e^\pm})}. \quad (30)$$

$T(r)$ is the local gas temperature and η_{e^\pm} the degeneracy parameter of electrons or positrons, defined as the ratio of the chemical potential to the temperature. A factor of 2 was taken into account as the statistical weight for positive and negative spin states. Inserting Eq. (30) into Eq. (29) one gets for the cooling rate per unit volume

$$Q_\nu^- = (3\alpha^2 + 1) \frac{\pi \sigma_0 c (kT)^6}{(hc)^3 (m_e c^2)^2} \frac{\rho}{m_u} \\ \times [Y_p \mathcal{F}_5(\eta_e) + Y_n \mathcal{F}_5(-\eta_e)] \\ \approx 145 \frac{\rho}{m_u} \left(\frac{kT}{2 \text{ MeV}}\right)^6 \left[\frac{\text{MeV}}{\text{s}}\right], \quad (31)$$

where the numerical factor is the rate in MeV per nucleon when $Y_n + Y_p \approx 1$ and the equilibrium relation $\eta_{e^-} = -\eta_{e^+} \equiv \eta_e$ with $\eta_e \approx 0$ are used. The latter approximation is good in the shock-heated layers because the electron fraction $Y_e = n_e/n_b$ and thus the electron degeneracy is rather low and e^\pm pairs are abundant. $\mathcal{F}_5(\eta)$ is the Fermi integral for relativistic particles,

$$\mathcal{F}_j(\eta) = \int_0^\infty dx \frac{x^j}{1 + \exp(x - \eta)}, \quad (32)$$

with $\mathcal{F}_5(0) \approx 118$. (Useful formulae for sums and differences of these Fermi integrals can be found in Bludman & Van Riper, 1978, and simple approximations in Takahashi et al. 1978.)

Heating balances cooling at the gain radius, i.e., the gain radius R_g has to fulfill the condition $Q_\nu^+ = Q_\nu^-$ by definition. With Eqs. (28) and (31) one obtains the following relation:

$$R_{g,7} \left(\frac{kT_g}{2 \text{ MeV}}\right)^3 \approx 1.05 \sqrt{\frac{L_{\nu_e,52}}{\langle\mu_\nu\rangle_g}} \left(\frac{kT_{\nu_e}}{4 \text{ MeV}}\right). \quad (33)$$

$R_{g,7}$ is the gain radius in units of 10^7 cm and $T_g = T(R_g)$ the temperature at the gain radius. Depending on the position of the gain radius, $\langle\mu_\nu\rangle_g$ is a factor somewhere between 0.25 (value at the neutrinosphere) and unity (limit for $r \rightarrow \infty$).

4.3. The EoS transition radius

It is interesting to consider the conditions for which the pressure is dominated by nonrelativistic nucleons or radiation plus relativistic e^\pm pairs ($kT \gtrsim 0.5$ MeV). In the first case $P \approx P_b = kT\rho/m_u$, if nuclei are fully dissociated into free nucleons. In the latter case $P \approx P_r = P_{e^\pm} + P_\gamma \approx \frac{11}{12} a_\gamma (kT)^4$, when $\eta_e \approx 0$ is again assumed for the electron degeneracy and the constant is $a_\gamma = 8\pi^5/[15(hc)^3] \approx 8.56 \times 10^{31} \text{ MeV}^{-3} \text{ cm}^{-3}$. Setting P_b equal to P_r gives

$$\frac{(kT)^3}{\rho} = \frac{12}{11} \frac{1}{m_u a_\gamma} \quad (34)$$

or, using the temperature $kT \approx kT_{\nu_e} \approx 4$ MeV (compare Fig. 2),

$$\left(\frac{kT}{4 \text{ MeV}}\right)^3 \rho_{10}^{-1} \cong 1.2. \quad (35)$$

This means that the transition from the baryon-dominated to the radiation-dominated regime occurs at a density significantly below that of the neutrinosphere. The latter is typically above 10^{11} g/cm^3 . When the electron degeneracy is negligibly small, the contributions of relativistic and nonrelativistic gas components to the pressure are equal for a value of the radiation entropy per nucleon of $s_r = s_{e^\pm} + s_\gamma \approx (\epsilon_r + P_r)/(kT\rho/m_u) = 4P_r/P_b = 4$. Here $\epsilon_r = 3P_r$ was used for the energy density of the relativistic particles.

4.4. The shock radius and infall region

Conservation of the mass flow, momentum flow and energy flow across the discontinuity of the shock front is expressed by the three Rankine-Hugoniot conditions

$$\rho_p u_p = \rho_s u_s, \quad (36)$$

$$P_p + \rho_p u_p^2 = P_s + \rho_s u_s^2, \quad (37)$$

$$\frac{1}{2} u_p^2 + w_p - q_d = \frac{1}{2} u_s^2 + w_s, \quad (38)$$

where the indices p and s denote quantities just ahead and behind the shock, respectively (see Fig. 2), $w = (\varepsilon + P)/\rho$ is the enthalpy per unit mass, q_d the nuclear binding energy per unit mass absorbed by photodisintegration of nuclei within the shock front, and $u = v - U_s$ the fluid velocity relative to the shock when $U_s = \dot{R}_s$ is the shock velocity and v the gas velocity relative to the center of the star. Note that in the infall region v has negative sign.

With the definition $\beta \equiv \rho_s/\rho_p$, Eq. (36) gives $u_s = u_p/\beta$, which can be used to eliminate u_s from Eq. (37). For a strong shock, i.e., $P_s \gg P_p$, this yields

$$P_s \approx \left(1 - \frac{1}{\beta}\right) \rho_p (v_p - U_s)^2. \quad (39)$$

Combining Eqs. (36)–(38) one further finds

$$w_s - w_p = \frac{1}{2} (P_s - P_p) \left(\frac{1}{\rho_s} + \frac{1}{\rho_p}\right) - q_d. \quad (40)$$

With $P_p \ll P_s$, $w_p \ll w_s$ and $w_s \approx 4P_s/\rho_s$ for the radiation-dominated gas in the postshock region, Eq. (40) can be rewritten as

$$\frac{\rho_s}{\rho_p} \approx 7 + \frac{2q_d \rho_s}{P_s} \approx \frac{7}{4 - 3\sqrt{1 + 14q_d/(9u_p^2)}}, \quad (41)$$

where in the second transformation Eq. (39) was used to replace P_s/ρ_s . This shows that for a relativistic gas the density jump in a strong shock is a factor of 7. Energy consumed by photodissociation of nuclei increases the density contrast between preshock and postshock region (Thompson 2000). In a more general treatment, retaining w_p and taking into account the (subdominant) contributions from nonrelativistic nucleons to the gas pressure behind the shock (but still using $P_p \ll \rho_p u_p^2$ in the infall region) one also derives the right hand side of Eq. (41), now with the expression

$$q^* \equiv q_d - w_p - \frac{3}{2m_u} \sum_i Y_i kT_s \quad (42)$$

instead of q_d in the denominator. This means that the density discontinuity is also affected by the preshock enthalpy and the thermal pressure of nucleons and nuclei behind the shock (the nuclear composition is accounted

for by the sum of the number fractions, $\sum_i Y_i$). Considering q_d to be several MeV/ m_u , $kT_s \sim 1$ MeV, and the preshock medium to be dominated by relativistic, degenerate electrons in which case $w_p \approx \zeta_e Y_e/m_u$ with an electron chemical potential $\zeta_e = \eta_e kT$ of a few MeV, one can see that all terms in Eq. (42) are of the same order and therefore equally important.

The preshock region is not affected by the postshock conditions. Because the shock moves supersonically relative to the medium ahead of it, sound waves cannot transport information in this direction. The matter there falls into the shock with a significant fraction of the free-fall velocity,

$$v_p = -\alpha \sqrt{\frac{2GM}{R_s}} \quad (43)$$

with $\alpha \sim 1/\sqrt{2}$ (Bethe 1990, 1993; Bruenn 1993). Ahead of the shock free nucleons are absent and therefore ν_e and $\bar{\nu}_e$ absorption does not play a role, but neutrinos interact with nuclei by coherent scatterings. The opacity of the latter reaction scales roughly with N^2/A when N is the neutron number and A the mass number of the nuclei, and the total neutrino opacity of the preshock medium turns out to be close to the result of Eq. (12). Therefore the momentum transfer by neutrinos was again taken into account by using \widetilde{M} instead of M in Eq. (43). Plugging Eq. (43) into the rate at which mass falls into the shock, $\dot{M} = 4\pi R_s^2 \rho_p v_p (< 0)$, gives the density just above the shock:

$$\rho_p = -\frac{\dot{M}}{4\pi \alpha \sqrt{2GM} R_s^{3/2}}. \quad (44)$$

On the other hand, if the original presupernova material has a density distribution $\rho_0(r_0) = H r_0^{-3}$ with H being a constant, then mass conservation yields a density at the footpoint of the shock at time t after the start of the collapse of

$$\rho_p = \frac{2}{3} \frac{H}{\alpha \sqrt{2GM}} t^{-1} R_s^{-3/2} \quad (45)$$

(Bethe 1990, 1993; see also Cooperstein et al. 1984). Comparing Eqs. (44) and (45) one finds that the rate at which mass crosses the shock in this case is

$$\dot{M} = -\frac{8\pi}{3} \frac{H}{t}, \quad (46)$$

which depends on the structure of the progenitor star through the constant H and decreases with time.

5. Structure of the atmosphere

Within the supernova shock, the infalling matter is strongly decelerated to a velocity $v_s = (v_p - U_s)/\beta + U_s$.

For a stalled shock, $|v_s| \ll |v_p|$. Compared to the internal energy and the gravitational energy, the kinetic energy behind the shock is therefore negligibly small. The gas is further slowed down as it moves inward and settles onto the nascent neutron star. Between neutrinosphere and shock front $dv/dt \approx 0$ is therefore a good assumption, i.e., the stellar structure is well approximated by hydrostatic equilibrium (Chevalier 1989; Bethe 1993, 1995; Fryer et al. 1996). Combining Eqs. (2) and (3) and using Eq. (6), the equation of hydrostatic equilibrium is found to be

$$-\frac{1}{\rho} \frac{\partial P}{\partial r} - \frac{G \widetilde{M}}{r^2} = 0. \quad (47)$$

In the following, the solutions of this equation in the layers between neutrinosphere R_ν and EoS transition radius R_{eos} and between R_{eos} and shock position R_s will be derived.

5.1. Hydrostatic equilibrium between R_ν and R_{eos}

When nonrelativistic baryons dominate the pressure and relativistic electrons contribute, but positrons and radiation can be ignored because the electrons are mildly degenerate, the pressure can be expressed as

$$P \approx P_b + P_{e^-} = \frac{\rho}{m_u} kT \left(1 + \frac{Y_e}{3} \frac{\mathcal{F}_3(\eta_e)}{\mathcal{F}_2(\eta_e)} \right) \equiv f_g \frac{\rho}{m_u} kT. \quad (48)$$

Since Y_e and the electron degeneracy do not vary strongly, the factor f_g can be considered as constant. Between R_ν and R_{eos} also the temperature is a slowly changing quantity, $T(r) \approx T_\nu \approx T_{\nu_e}$ (compare Fig. 2). Hydrostatic equilibrium therefore implies

$$\rho(r) = \rho_\nu \exp \left[-\frac{G \widetilde{M} m_u}{f_g k T_\nu R_\nu} \left(1 - \frac{R_\nu}{r} \right) \right], \quad (49)$$

where ρ_ν is the density at the neutrinosphere. Near the neutrinosphere, $r \approx R_\nu$, this can be approximated by

$$\rho(r) \approx \rho_\nu \exp \left(-\frac{x}{h} \right) \quad (50)$$

$$\text{with } x \equiv r - R_\nu \text{ and } h \equiv f_g \frac{k T_\nu R_\nu^2}{G \widetilde{M} m_u}.$$

Using typical numbers gives

$$h \approx 2.9 \times 10^4 f_g R_{\nu,6}^2 \left(\frac{k T_\nu}{4 \text{ MeV}} \right) \left(\frac{\widetilde{M}}{M_\odot} \right)^{-1} \text{ [cm]}, \quad (51)$$

where $R_{\nu,6}$ is the radius of the neutrinosphere in units of 10^6 cm.

The density declines exponentially outside the neutrinosphere with a scale height $h \ll r$, forming a sharp ‘‘cliff’’ (Bethe & Wilson 1985, Bethe 1990, Woosley 1993). For

this reason the effective optical depth is dominated by the immediate vicinity of the neutrinosphere. Therefore the integration in Eq. (13) can be performed, using Eq. (50) for the density in the effective opacity of Eq. (16), to derive the neutrinospheric density (normalized to 10^{10} g/cm³) as

$$\rho_{\nu,10} \approx 150 f_g^{-1} R_{\nu,6}^{-2} \left(\frac{\widetilde{M}}{M_\odot} \right) \left(\frac{k T_\nu}{4 \text{ MeV}} \right)^{-3}. \quad (52)$$

This result confirms that the density of the transition from the baryon-dominated to the radiation-dominated regime [Eq. (35)] is significantly lower than ρ_ν .

5.2. Hydrostatic equilibrium between R_{eos} and R_s

In the radiation-dominated region a large part of the pressure is due to relativistic electron-positron pairs and photons, but also contributions from nucleons and nuclei with number fractions Y_i might not be negligible, therefore

$$\begin{aligned} P &= P_\gamma + P_{e^\pm} + P_b \\ &= \frac{a_\gamma}{3} (kT)^4 \left[\frac{11}{4} + \frac{15}{2\pi^4} \eta_e^2 \left(\pi^2 + \frac{\eta_e^2}{2} \right) + \frac{3\rho kT \sum_i Y_i}{m_u a_\gamma (kT)^4} \right] \\ &\equiv P_r \left(1 + \frac{4}{g_r s_\gamma} \right) \equiv f_r P_r, \end{aligned} \quad (53)$$

where P_r is the pressure associated with relativistic particles,

$$P_r = g_r P_\gamma = \frac{1}{3} a_\gamma g_r (kT)^4, \quad (54)$$

$$\text{with } g_r \equiv \frac{11}{4} + \frac{15}{2\pi^4} \eta_e^2 \left(\pi^2 + \frac{1}{2} \eta_e^2 \right), \quad (55)$$

s_γ is the entropy per nucleon carried by photons, $s_\gamma = 4a_\gamma (kT)^3 / (3\rho/m_u)$, and $\sum_i Y_i \approx 1$ because of the nearly complete disintegration of nuclei. If both the factor g_r and s_γ are constant (which is roughly fulfilled in the radiation-dominated region between R_{eos} and R_s where the electron degeneracy parameter η_e is small, and, as was discussed in Sect. 2, convective processes tend to homogenize the total entropy and thus also the radiation entropy; see Bethe 1996b) then also f_r can be considered as constant. In this case the pressure is simply proportional to $(kT)^4$, both for the contribution from nucleons and for the contribution from photons plus electron-positron pairs (for a detailed discussion, see Bethe 1993).

This implies that the density ρ is proportional to T^3 , i.e.,

$$P = f_r g_r \frac{a_\gamma}{3} (kT)^4 = K \rho^{4/3}. \quad (56)$$

Note that Eq. (56) is valid more generally than for radiation-dominated conditions (Bethe 1996b). Using

$$n_e = Y_e \frac{\rho}{m_u} = \frac{8\pi}{3} \frac{(kT)^3}{(hc)^3} \eta_e (\pi^2 + \eta_e^2), \quad (57)$$

the coefficient K can be determined as

$$K = f_{\text{r}g_{\text{r}}} \frac{a_{\gamma}}{3} (hc)^4 \left(\frac{3}{8\pi} \frac{Y_e}{m_{\text{u}} \eta_e (\pi^2 + \eta_e^2)} \right)^{4/3}. \quad (58)$$

If K in Eq. (58) is approximately constant, which is typically fulfilled in the region between R_{g} and R_{s} (Bethe 1996b), Eq. (56) is a useful representation of the equation of state.

With Eq. (47), one can now determine the density distribution between R_{eos} and R_{s} in hydrostatic equilibrium as

$$\rho(r) = \left[\rho_{\text{s}}^{1/3} + \frac{1}{4} \frac{G \widetilde{M}}{K} \left(\frac{1}{r} - \frac{1}{R_{\text{s}}} \right) \right]^3. \quad (59)$$

Inserting this in Eq. (56) and setting $K = P_{\text{s}}/\rho_{\text{s}}^{4/3}$, the pressure as a function of radius is obtained,

$$P(r) = \left[P_{\text{s}}^{1/4} + \frac{1}{4} \frac{G \widetilde{M}}{K^{3/4}} \left(\frac{1}{r} - \frac{1}{R_{\text{s}}} \right) \right]^4, \quad (60)$$

and $kT(r)$ can also be found from Eq. (56) as

$$kT(r) = kT_{\text{s}} + \frac{1}{4} \left(\frac{3}{f_{\text{r}g_{\text{r}}} a_{\gamma}} \right)^{1/4} \frac{G \widetilde{M}}{K^{3/4}} \left(\frac{1}{r} - \frac{1}{R_{\text{s}}} \right) \quad (61)$$

when $kT_{\text{s}} = [3P_{\text{s}}/(f_{\text{r}g_{\text{r}}} a_{\gamma})]^{1/4}$ is used. If the density-pressure relation is more general than Eq. (56), namely $P = K\rho^{\gamma}$ with K being constant, hydrostatic equilibrium implies

$$\rho(r) = \left[\rho_{\text{s}}^{\gamma-1} + \frac{\gamma-1}{\gamma} \frac{G \widetilde{M}}{K} \left(\frac{1}{r} - \frac{1}{R_{\text{s}}} \right) \right]^{1/(\gamma-1)}, \quad (62)$$

which replaces Eq. (59).

Instead of the general solutions, Eqs. (59)–(61), simple power-laws,

$$\begin{aligned} \rho(r) &= \rho_{\text{s}} \left(\frac{R_{\text{s}}}{r} \right)^3, \quad kT(r) = kT_{\text{s}} \frac{R_{\text{s}}}{r}, \\ P(r) &= P_{\text{s}} \left(\frac{R_{\text{s}}}{r} \right)^4, \end{aligned} \quad (63)$$

yield a good approximation for the hydrostatic atmosphere, if K fulfills the condition $K = G\widetilde{M}/(4R_{\text{s}}\rho_{\text{s}}^{1/3})$. Since $K = P_{\text{s}}/\rho_{\text{s}}^{4/3}$, this is equivalent to the requirement that

$$\frac{P_{\text{s}}}{\rho_{\text{s}}} = \frac{G \widetilde{M}}{4 R_{\text{s}}}. \quad (64)$$

On the other hand, from Eqs. (39) and (43) one gets

$$\begin{aligned} \frac{P_{\text{s}}}{\rho_{\text{s}}} &\approx \frac{\beta-1}{\beta^2} \frac{2\alpha^2 G \widetilde{M}}{R_{\text{s}}} \left(1 - \frac{U_{\text{s}}}{v_{\text{p}}} \right)^2 \\ &\sim \frac{6}{49} \frac{G \widetilde{M}}{R_{\text{s}}} \left(1 - \frac{U_{\text{s}}}{v_{\text{p}}} \right)^2. \end{aligned} \quad (65)$$

The numerical factor on the right hand side of Eq. (65) was obtained with $\alpha \sim 1/\sqrt{2}$ (Bethe 1990, 1993) and $\beta \sim 7$ [Eq. (41)]. Equation (65) shows that the requirement of Eq. (64) is reasonably well, although for small shock radii not very well, fulfilled. In the following the power-laws of Eq. (63) will therefore only serve to facilitate analytical evaluation, and the use of this approximate solution of hydrostatic equilibrium will be avoided where inconsistencies might result.

With Eqs. (33) and (63) the gain radius R_{g} and the conditions at the gain radius can be expressed in terms of the properties at the shock front and the characteristic parameters (T_{ν_e} , L_{ν_e}) of the neutrino emission. Inserting the relation $kT_{\text{g}} = kT_{\text{s}}(R_{\text{s}}/R_{\text{g}})$ into Eq. (33) yields the gain radius (in units of 10^7 cm),

$$R_{\text{g},7} \approx 0.98 R_{\text{s},7}^{\frac{3}{2}} (kT_{\text{s},2})^{\frac{3}{2}} (kT_{\nu_e,4})^{-\frac{1}{2}} \left(\frac{L_{\nu_e,52}}{\langle \mu_{\nu} \rangle_{\text{g}}} \right)^{-\frac{1}{4}}, \quad (66)$$

and for the temperature at the gain radius one gets

$$kT_{\text{g},2} \approx 1.02 R_{\text{s},7}^{-\frac{1}{2}} (kT_{\text{s},2})^{-\frac{1}{2}} (kT_{\nu_e,4})^{\frac{1}{2}} \left(\frac{L_{\nu_e,52}}{\langle \mu_{\nu} \rangle_{\text{g}}} \right)^{\frac{1}{4}}, \quad (67)$$

where $kT_{\text{g},2} = kT_{\text{g}}/(2 \text{ MeV})$ and $kT_{\nu_e,4}$ is the neutrinospheric temperature and $kT_{\text{s},2}$ the postshock temperature normalized to 4 MeV and 2 MeV, respectively.

The assumptions made in this section to solve the equation of hydrostatic equilibrium in the layer between R_{eos} and R_{s} do not seem to be very restrictive, because two-dimensional as well as one-dimensional simulations without convection (e.g., Bruenn 1993; Janka & Müller 1996, Fig. 6; Rampp 2000) yield density and temperature profiles in the postshock region which are very close to power laws with power law indices around 3 and 1, respectively. Near R_{eos} the contributions of relativistic and nonrelativistic gas components will become equally important. Here the exponentially steep density decline just outside the neutrinosphere must change to the power-law behavior behind the shock, and both of these limiting solutions will not provide a good description. The exact structure in the intermediate layer between R_{eos} and R_{g} , however, does not play an important role in the further discussion and therefore a more accurate treatment is not necessary.

6. Heating and cooling

To discuss energy deposition and emission of neutrinos exterior to the neutrinosphere, one starts with the energy equation for ν_e plus $\bar{\nu}_e$, which is

$$\frac{1}{4\pi r^2} \frac{\partial L_{\nu}}{\partial r} = -Q_{\nu}^{+} + Q_{\nu}^{-}, \quad (68)$$

where $L_{\nu} = L_{\nu_e} + L_{\bar{\nu}_e}$ and Q_{ν}^{+} and Q_{ν}^{-} are the heating and cooling rates of the stellar medium as given by

Eqs. (28) and (31), respectively. In writing Eq. (68), stationarity was assumed for the neutrinos, which is justified because the neutrino emission of the accreting neutrino star changes on a timescale which is typically longer than other relevant timescales of the discussed problem. From Eq. (68) the net effect of heating or cooling in a layer between radii r_1 and r_2 can be deduced as

$$\int_{r_1}^{r_2} dr 4\pi r^2 (Q_\nu^+ - Q_\nu^-) = L_\nu(r_1) - L_\nu(r_2). \quad (69)$$

Referring to Eqs. (23) and (27), a suitable spectral and flavor average for the absorption coefficient of ν_e and $\bar{\nu}_e$ can be defined as

$$\langle \kappa_a \rangle = \frac{Q_\nu^+}{L_\nu / (4\pi r^2 \langle \mu_\nu \rangle)}, \quad (70)$$

when $\langle \mu_{\nu_e} \rangle \approx \langle \mu_{\bar{\nu}_e} \rangle \equiv \langle \mu_\nu \rangle$ is used. Plugging this into Eq. (68) gives

$$\frac{\partial L_\nu}{\partial r} = -\langle \kappa_a \rangle \frac{L_\nu}{\langle \mu_\nu \rangle} + 4\pi r^2 Q_\nu^-. \quad (71)$$

The neutrino luminosity as a function of radius $r \geq r_0$ is the general solution of Eq. (71):

$$L_\nu(r) = \exp \left\{ -\int_{r_0}^r dr' \frac{\langle \kappa_a \rangle}{\langle \mu_\nu \rangle} \right\} L_\nu(r_0) + \int_{r_0}^r dr' 4\pi (r')^2 Q_\nu^- \exp \left\{ -\int_{r'}^r dr'' \frac{\langle \kappa_a \rangle}{\langle \mu_\nu \rangle} \right\}. \quad (72)$$

The first exponential factor represents the absorption damping of the luminosity in the shell between r_0 and r , the second exponential factor the reabsorption of neutrinos emitted at r' in the layer enclosed by radii r' and r .

6.1. Heating and cooling between R_ν and R_g

Here the lower boundary of the considered volume is the neutrinosphere at radius $r_0 = R_\nu$. Since both $\langle \kappa_a \rangle \propto \rho(r)$ [cf. Eqs. (70) and (28)] and $Q_\nu^- \propto \rho(r)$ [cf. Eq. (31)] are steep functions of the radius in the region between R_ν and R_g , where the density drops exponentially, most of the absorption and emission occurs in the immediate vicinity of the neutrinosphere. Therefore the neutrino luminosity at the gain radius, $L_\nu(R_g)$, can be approximated by the limit for $r \rightarrow \infty$ of Eq. (72), and the integral $\int_{r'}^r dr'' \langle \kappa_a \rangle / \langle \mu_\nu \rangle$ can be replaced by $\int_{R_\nu}^\infty dr \langle \kappa_a \rangle / \langle \mu_\nu \rangle$. This leads to

$$L_\nu(R_g) \approx \exp \left\{ -\int_{R_\nu}^\infty dr \frac{\langle \kappa_a \rangle}{\langle \mu_\nu \rangle} \right\} \times \left[L_\nu(R_\nu) + \int_{R_\nu}^\infty dr 4\pi r^2 Q_\nu^- \right]. \quad (73)$$

To evaluate the exponential damping factor, $\langle \kappa_a \rangle$ is expressed by Eq. (70), making use of Eq. (28) and $L_\nu = 2L_{\nu_e}$. The neutrino spectrum is assumed not to change outside the neutrinosphere. With Eq. (50) the integral over the density profile becomes $\int_{R_\nu}^\infty dr \rho(r) \approx \rho_\nu h$. Employing Eqs. (51) and (52), one finds

$$\int_{R_\nu}^\infty dr \frac{\langle \kappa_a \rangle}{\langle \mu_\nu \rangle} \approx \frac{0.42}{\langle \mu_\nu \rangle} \equiv a, \quad (74)$$

where $\widetilde{\langle \mu_\nu \rangle}$ denotes a radial average of the flux factor $\langle \mu_\nu \rangle$ in the layer between R_ν and R_g . The energy loss integral is calculated with Eq. (31) where $T(r) \approx T_{\nu_e}$ is used near the neutrinosphere. With $\int_{R_\nu}^\infty dr r^2 \rho(r) \approx \rho_\nu h [h^2 + (R_\nu + h)^2] \approx \rho_\nu R_\nu^2 h$ [because $h \ll R_\nu$, cf. Eq. (51)] and Eqs. (51) and (52) this leads to:

$$\int_{R_\nu}^\infty dr 4\pi r^2 Q_\nu^- \approx 4.9 \times 10^{51} R_{\nu,6}^2 \left(\frac{kT_{\nu_e}}{4 \text{ MeV}} \right)^4 \left[\frac{\text{erg}}{\text{s}} \right] \equiv b. \quad (75)$$

Eq. (73) now becomes

$$L_\nu(R_g) \approx e^{-a} [L_\nu(R_\nu) + b], \quad (76)$$

and the total energy exchange between R_ν and R_g according to Eq. (69) therefore is

$$L_\nu(R_g) - L_\nu(R_\nu) \equiv L_{\text{acc}} \approx (e^{-a} - 1)L_\nu(R_\nu) + e^{-a}b. \quad (77)$$

Since R_g separates the layer of neutrino cooling from the one of neutrino heating, the region between R_ν and R_g must lose energy by neutrino emission. Therefore the neutrino luminosity at R_g must be larger than $L_\nu(R_\nu)$, and L_{acc} represents the luminosity associated with the accretion of matter through the gain radius onto the surface of the nascent neutron star. The requirement $L_{\text{acc}} \geq 0$ constrains the luminosity of the neutron star core relative to the product $R_\nu^2 (kT_{\nu_e})^4$ by the inequality

$$L_\nu(R_\nu) \leq b (e^a - 1)^{-1}. \quad (78)$$

Provided the core luminosity can be expressed in terms of blackbody emission of temperature T_{ν_e} ,

$$L_\nu(R_\nu) \approx 4\pi R_\nu^2 \frac{c}{4} \frac{7}{8} a_\gamma (kT_{\nu_e})^4 \approx 2.9 \times 10^{51} R_{\nu,6}^2 \left(\frac{kT_{\nu_e}}{4 \text{ MeV}} \right)^4 \left[\frac{\text{erg}}{\text{s}} \right], \quad (79)$$

the consistency condition translates into the relation

$$\widetilde{\langle \mu_\nu \rangle} \gtrsim 0.42, \quad (80)$$

which is satisfied above the neutrinosphere in the layer between R_ν and R_g .

6.2. Heating and cooling between R_g and R_s

For reasons of simplicity it will be assumed that in the layer bounded by R_g and R_s nuclei are completely disintegrated into free nucleons. Disregarding the occurrence of α particles, in particular, is certainly an approximation which becomes invalid when the temperature drops below about 1 MeV, i.e., when the shock is at large radii, typically around 300 km (see Bethe 1993, 1995, 1996a,b,c, 1997). The presence of α particles reduces the neutrino heating, because electron neutrinos and antineutrinos are absorbed only on nucleons, but energy released by the recombination of α 's during shock expansion supports the shock at a later stage and contributes to the energy budget of the explosion. Since in the context of this paper we do not attempt to calculate the explosion energy, but are interested in a qualitative discussion of the revival phase of the stalled shock, the recombination of nucleons to α particles is probably not a crucial issue.

As will be demonstrated below, the optical depth between R_g and R_s is small such that $\int_{R_g}^{R_s} dr \langle \kappa_a \rangle / \langle \mu_\nu \rangle \lesssim 0.5$. Therefore the reabsorption probability of emitted neutrinos is also small and an approximation to the solution of Eq. (72) at the shock position is

$$L_\nu(R_s) \approx \left(1 - \int_{R_g}^{R_s} dr \frac{\langle \kappa_a \rangle}{\langle \mu_\nu \rangle} \right) L_\nu(R_g) + \int_{R_g}^{R_s} dr 4\pi r^2 Q_\nu^-. \quad (81)$$

The net energy deposition is found to be

$$\begin{aligned} L_\nu(R_g) - L_\nu(R_s) &\approx \int_{R_g}^{R_s} dr \frac{\langle \kappa_a \rangle}{\langle \mu_\nu \rangle} L_\nu(R_g) - \int_{R_g}^{R_s} dr 4\pi r^2 Q_\nu^- \\ &\equiv \mathcal{H} - \mathcal{C}. \end{aligned} \quad (82)$$

Since in the layer bounded by R_g and R_s neutrino heating takes place, $L_\nu(R_g) \geq L_\nu(R_s)$ (this will also be verified below). Expanding the exponential damping factors only to lowest order in the exponent implies a slight overestimation of the energy input into the stellar medium by neutrinos (because the luminosity entering at R_g is assumed to decay linearly through the layer), but also the energy loss by neutrinos is overestimated, because the reabsorption of emitted neutrinos is not included.

Using Q_ν^+ from Eq. (28) in Eq. (70), $L_\nu = 2L_{\nu_e}$, and the density profile from Eq. (63), one finds for the first integral in Eq. (82):

$$\begin{aligned} \mathcal{H} &\approx 4.9 \times 10^{50} \frac{L_{\nu,52}(R_g)}{\langle \mu_\nu \rangle^*} (kT_{\nu_e,4})^2 \rho_{s,9} R_{s,7} \\ &\quad \times \left[\left(\frac{R_s}{R_g} \right)^2 - 1 \right] \left[\frac{\text{erg}}{\text{s}} \right], \end{aligned} \quad (83)$$

where kT_{ν_e} was again treated as a constant, $\langle \mu_\nu \rangle^*$ defines an average value of the flux factor in the layer between R_g

and R_s , and $\rho_{s,9}$ is the density behind the shock in units of 10^9 g cm^{-3} . The second integral in Eq. (82) is evaluated with Q_ν^- from Eq. (31) and the temperature and density relations from Eq. (63):

$$\begin{aligned} \mathcal{C} &\approx 2.9 \times 10^{50} (kT_{s,2})^6 \rho_{s,9} R_{s,7}^3 \\ &\quad \times \left[\left(\frac{R_s}{R_g} \right)^6 - 1 \right] \left[\frac{\text{erg}}{\text{s}} \right]. \end{aligned} \quad (84)$$

Employing the gain condition, Eq. (33), and again making use of Eq. (63), one gets

$$\left(\frac{kT_s}{2 \text{ MeV}} \right)^6 \approx 0.55 \frac{L_{\nu,52}(R_g)}{\langle \mu_\nu \rangle_g R_{g,7}^2} \left(\frac{kT_{\nu_e}}{4 \text{ MeV}} \right)^2 \left(\frac{R_g}{R_s} \right)^6, \quad (85)$$

which serves to rewrite Eq. (84) as

$$\begin{aligned} \mathcal{C} &\approx 1.6 \times 10^{50} \frac{L_{\nu,52}(R_g)}{\langle \mu_\nu \rangle_g} (kT_{\nu_e,4})^2 \rho_{s,9} R_{s,7} \\ &\quad \times \left(\frac{R_s}{R_g} \right)^2 \left[1 - \left(\frac{R_g}{R_s} \right)^6 \right] \left[\frac{\text{erg}}{\text{s}} \right]. \end{aligned} \quad (86)$$

Combining Eqs. (83) and (86) gives the net energy transfer to the stellar medium in the gain region:

$$\mathcal{H} - \mathcal{C} \approx \mathcal{H} \times \left\{ 1 - \frac{1}{3} \frac{\langle \mu_\nu \rangle^*}{\langle \mu_\nu \rangle_g} \left[1 + \left(\frac{R_g}{R_s} \right)^2 + \left(\frac{R_g}{R_s} \right)^4 \right] \right\}. \quad (87)$$

Since $\langle \mu_\nu \rangle^* / \langle \mu_\nu \rangle_g \sim 1$ and $R_s > R_g$, typically $R_s \sim 2R_g$, we verify that $\mathcal{H} - \mathcal{C} > 0$ and therefore $L_\nu(R_s) < L_\nu(R_g)$, as expected for the neutrino heating region. For $\beta = \rho_s / \rho_p \approx 7$ [Eq. (41)] and $\alpha = 1/\sqrt{2}$, Eq. (44) yields for the postshock density

$$\rho_s \approx 3 \times 10^9 \frac{(-\dot{M})}{M_\odot / \text{s}} \left(\frac{\widetilde{M}}{M_\odot} \right)^{-1/2} R_{s,7}^{-3/2} \left[\frac{\text{g}}{\text{cm}^3} \right]. \quad (88)$$

Using this and $R_s \sim 2R_g$ in Eq. (83) leads to

$$\begin{aligned} \int_{R_g}^{R_s} dr \frac{\langle \kappa_a \rangle}{\langle \mu_\nu \rangle} &= \frac{\mathcal{H}}{L_\nu(R_g)} \\ &\sim \frac{0.44}{\langle \mu_\nu \rangle^*} \frac{(kT_{\nu_e,4})^2}{R_{s,7}^{1/2}} \frac{(-\dot{M})}{M_\odot / \text{s}} \left(\frac{\widetilde{M}}{M_\odot} \right)^{-\frac{1}{2}}. \end{aligned} \quad (89)$$

For sufficiently small accretion rates $|\dot{M}|$ this is less than about 0.5, and the assumption made before Eq. (81) is verified, i.e., the reabsorption of neutrinos emitted in the gain region can be neglected.

7. Mass accretion onto the neutron star

The shock accretes mass at a rate $\dot{M} \equiv 4\pi R_s^2 \rho_p v_p$ as determined by the conditions in the core of the progenitor

star (see Sect. 4.4). In a stationary state, this rate is equal to the rate at which matter is advected inward from the shock to the neutrinosphere to be finally added into the neutron star. The rate at which matter can be absorbed by the neutron star, however, depends on the efficiency by which neutrinos are able to remove the energy excess of the infalling material relative to the energy of the strongly bound matter in the neutron star surface layers. For the large accretion rates typical of the collapsed stellar core right after bounce, the density is so high that the infalling matter becomes opaque to neutrinos. In this case the efficiency of the energy loss is reduced. When the gas is hotter, the neutrino opacity increases (because of the energy dependence of the neutrino cross sections), and the neutrinosphere moves to a larger radius. Due to this regulatory effect, the neutrinospheric temperature is a rather inert quantity and, e.g., turns out to be very similar in different numerical models. Therefore it is not a steady-state mass accretion rate which governs the temperature at the base of the “atmosphere” (as for accretion in optically thin conditions), but the “surface” of the nascent neutron star forms where the temperature is sufficiently high for neutrino opaqueness to set in.

When neutrino cooling is not efficient enough, the advection of matter through the neutrino cooling region is reduced compared to the accretion into the shock, and matter piles up on top of the neutron star. Similarly, strong neutrino heating in the gain region can reduce the inflow of matter. The transition from accretion to an explosion is characterized by an inversion of infall to outflow. For this reason the analysis of the conditions for shock revival requires the inclusion of this sort of time-dependence in the discussion. In the simplified model considered here, the mass accretion rate is allowed to change between R_s and R_g . Matter advected through R_g at a rate determined by the efficiency of neutrino cooling is then assumed to be added into the neutron star (compare Fig. 2).

Using Eqs. (2) and (6) and the definition $\dot{M}(r) = 4\pi r^2 \rho v$, Eq. (4) can be rewritten in the following form:

$$\begin{aligned} \frac{\partial}{\partial r} \left[\dot{M} \left(\frac{e+P}{\rho} - \frac{G\widetilde{M}}{r} \right) \right] &= 4\pi r^2 (Q_\nu + Q_d) \\ &- 4\pi r^2 \rho \frac{\partial}{\partial t} \left(\frac{e}{\rho} \right) \\ &+ \left(\frac{e}{\rho} - \frac{G\widetilde{M}}{r} \right) \frac{\partial \dot{M}}{\partial r}, \end{aligned} \quad (90)$$

where $Q_\nu = Q_\nu^+ - Q_\nu^-$ is the net rate (per unit volume) of energy transfer between neutrinos and the stellar medium and Q_d denotes the energy consumed or released by the photodisintegration of nuclei. The latter term has to be introduced in the equation when rest-mass contributions from nucleons and nuclei are not included in the internal energy density ε [Eq. (5)]. The nuclei present in the accretion flow through the shock are assumed to be disso-

ciated to free nucleons within the shock front [cf. Eq. (38)]. Therefore the rate Q_d in terms of the (positive) nuclear binding energy per unit mass, q_d , is

$$Q_d = \rho v q_d \delta(r - R_s). \quad (91)$$

Here $\delta(x)$ is the delta function. For $v < 0$, which is true in case of accretion, energy is extracted from the stellar medium, i.e., $Q_d < 0$. Now integrating Eq. (90) between R_ν and a radius r that is infinitesimally larger than R_s gives

$$\begin{aligned} \dot{M} \left[\frac{e+P}{\rho} - \frac{G\widetilde{M}}{r} \right]_{R_s} - \dot{M}' \left[\frac{e+P}{\rho} - \frac{G\widetilde{M}}{r} \right]_{R_\nu} &= \\ \dot{M}' q_d + \int_{M(R_\nu)}^{M(R_s)} dM \left[\frac{Q_\nu}{\rho} - \frac{\partial}{\partial t} \left(\frac{e}{\rho} \right) \right] &+ \\ + \int_{\dot{M}'}^{\dot{M}} d\dot{M} \left(q_d + \frac{e}{\rho} - \frac{G\widetilde{M}}{r} \right), \end{aligned} \quad (92)$$

where $\partial M / \partial r = 4\pi r^2 \rho$ was used, the mass accretion rate through the neutrinosphere was defined as $\dot{M}' \equiv \dot{M}(R_\nu) = 4\pi R_\nu^2 \rho_\nu v_\nu$, and the term for the rate of energy consumption by nuclear dissociation was split into two parts according to $\dot{M}(r) = \dot{M}' + \int_{\dot{M}'}^{\dot{M}(r)} d\dot{M}$.

From Eq. (92) an approximation for \dot{M}' can be derived by taking into account that $|Q_\nu / \rho| \gg \partial(e/\rho) / \partial t$ in the region between R_ν and R_s , where strong neutrino heating and cooling occurs. Moreover, the integrand of the last term on the right hand side of Eq. (92) is usually small, because q_d corresponds to about 8–9 MeV per nucleon for complete disintegration of nuclei into free nucleons, $G\widetilde{M}/R_s \sim 14(\widetilde{M}/M_\odot)/R_{s,7}$ MeV per nucleon, and $e/\rho \approx \frac{1}{2}v_p^2 \sim \frac{1}{2}G\widetilde{M}/R_s$ immediately above the shock, where the infall velocity v_p is given by Eq. (43) and the specific internal energy is typically much smaller than the specific kinetic energy. For the same reason, the first term on the left hand side of Eq. (92) is much smaller than the second term when \dot{M} and \dot{M}' are of the same order. With all this one gets

$$\dot{M}' \approx - \int_{R_\nu}^{R_s} dr 4\pi r^2 Q_\nu \times \left(\left[\frac{e+P}{\rho} \right]_{R_\nu} - \frac{G\widetilde{M}}{R_\nu} + q_d \right)^{-1}. \quad (93)$$

Because of the large gravitational binding energy of matter at the neutrinosphere, the term in brackets in Eq. (93) is negative. The integral adds up the contributions from neutrino cooling between R_ν and R_g and from neutrino heating between R_g and R_s . If cooling is stronger (which is the case in the first second after bounce), the integral is negative and $\dot{M}' < 0$, i.e., the neutron star accretes matter. If neutrino heating dominates, there is mass outflow, $\dot{M}' > 0$. This is realized during the later phase of

the neutrino cooling evolution of the nascent neutron star, where a baryonic wind, the so-called neutrino-driven wind, is blown off the neutron star surface due to neutrino energy deposition just outside the neutrinosphere (Qian & Woosley 1996).

The integral in Eq. (93) was evaluated in Sect. 6:

$$\int_{R_\nu}^{R_s} dr 4\pi r^2 Q_\nu = -L_{\text{acc}} + \mathcal{H} - \mathcal{C}, \quad (94)$$

Equation (77) gives the net energy exchange between neutrinos and stellar medium in the layer $[R_\nu, R_g]$, Eq. (87) the corresponding result for the interval $[R_g, R_s]$, when \mathcal{H} is taken from Eq. (83) and the neutrino luminosity $L_\nu(R_g)$ from Eq. (76) with a and b provided by Eqs. (74) and (75), respectively. Plugging in numbers representative for the early post-bounce evolution, $L_\nu \approx 5 \times 10^{52} \text{ erg s}^{-1}$, $R_\nu \approx 50 \text{ km}$, $\widetilde{M} \approx 1 M_\odot$, $a \sim 1$, one finds $L_\nu(R_g) \approx 6.3 \times 10^{52} \text{ erg s}^{-1}$ and $\int_{R_\nu}^{R_g} dr 4\pi r^2 Q_\nu = -L_{\text{acc}} = L_\nu(R_\nu) - L_\nu(R_g) \approx -1.3 \times 10^{52} \text{ erg s}^{-1}$, and using $R_s \approx 2R_g \approx 200 \text{ km}$, $\langle \mu_\nu \rangle^* \sim 1$, $\langle \mu_\nu \rangle_g \sim 0.75$, yields $\int_{R_g}^{R_s} dr 4\pi r^2 Q_\nu = \mathcal{H} - \mathcal{C} \approx 7.7 \times 10^{51} \text{ erg s}^{-1}$. The gravitational energy at the neutrinosphere at 50 km is about -28 MeV per nucleon, q_d is roughly 8 MeV per nucleon, and the internal energy plus pressure account for typically $\sim 10 \text{ MeV}$ per nucleon:

$$\left(\frac{e + P}{\rho} \right)_{R_\nu} \approx \left(\frac{5}{2} + \frac{4}{3} Y_e \frac{\mathcal{F}_3(\eta_e)}{\mathcal{F}_2(\eta_e)} \right) \frac{kT_\nu}{m_u} \approx \frac{7}{2} \frac{kT_\nu}{m_u}, \quad (95)$$

where $e = \varepsilon$ has been applied because $\frac{1}{2}\rho v^2 \ll \varepsilon$ at the neutrinosphere. Therefore the sum of the terms in the denominator of Eq. (93) can be estimated to be about $-10^{19} \text{ erg g}^{-1}$. This leads to a mass accretion rate of the neutron star of $\dot{M}' \sim -0.3 M_\odot \text{ s}^{-1}$, a value which is in the range of the results of detailed numerical simulations and is of the order of the mass infall rate on the shock, \dot{M} .

8. Mass and energy conservation in the gain region

Mass and energy conservation in the gain region between R_g and R_s determine the early postbounce evolution of the supernova shock. For example, the shock is pushed outward when the matter that falls through the shock stays hot and piles up on top of the neutron star, forming an extended envelope instead of being accreted into the dense core quickly after efficient energy loss in the neutrino cooling layer below R_g . Similarly, strong neutrino heating in the gain region causes an increase of the postshock pressure and thus drives an expansion of the shock. On the other hand, enhanced neutrino emission will extract mass and/or energy from the layer which supports the supernova shock. The consequence will be a retraction of the shock in radius. These effects need to be accounted for by an appropriate discussion of the delayed explosion mechanism. A steady-state picture is certainly not adequate.

8.1. Mass in the gain region

The mass ΔM_g in the gain region can be calculated as volume integral over the density:

$$\Delta M_g = \int_{R_g}^{R_s} dr 4\pi r^2 \rho(r). \quad (96)$$

with the density $\rho(r)$ given by Eq. (59). Alternatively, since the latter equation is the exact solution for hydrostatic equilibrium, one can use $\rho(r) = -r^2(dP/dr)/(GM)$ with $P(r)$ from Eq. (60). Defining the coefficients $c_1 \equiv \rho_s^{1/3} - GM/(4KR_s)$ and $c_2 \equiv GM/(4K)$, one finds:

$$\begin{aligned} \Delta M_g &= 4\pi \left[\frac{1}{3} c_1 (R_s^3 - R_g^3) + \frac{3}{2} c_1^2 c_2 (R_s^2 - R_g^2) + \right. \\ &\quad \left. 3 c_1 c_2^2 (R_s - R_g) + c_2^3 \ln\left(\frac{R_s}{R_g}\right) \right] \\ &= 4\pi \left[\frac{1}{3} (R_s^3 \rho_s - R_g^3 \rho_g) + \frac{c_2}{2} (R_s^2 \rho_s^{2/3} - R_g^2 \rho_g^{2/3}) + \right. \\ &\quad \left. c_2^2 (R_s \rho_s^{1/3} - R_g \rho_g^{1/3}) + c_2^3 \ln\left(\frac{R_s}{R_g}\right) \right]. \quad (97) \end{aligned}$$

In deriving the second form of Eq. (97), use was made of $\rho(r) = (c_1 + c_2/r)^3$. Moreover, with $\rho = (P/K)^{3/4}$ the density in Eq. (97) can be substituted by the pressure P . Note that the quantities $\rho_g = \rho(R_g)$ and $P_g = P(R_g)$ at the gain radius must be expressed by the exact relations of Eqs. (59) and (60), respectively. They depend on the postshock state of the matter as do the coefficients c_1 and c_2 . The gain radius R_g is given by Eq. (66). It is also a function of the conditions immediately behind the shock. Writing the postshock temperature in terms of the postshock pressure via Eq. (56), $kT_s = [3P_s/(f_r g_r a_\gamma)]^{1/4}$, and using Eqs. (39), (43), (44) and (53)–(55) with typical values $\beta \sim 7$, $\alpha \sim 1/\sqrt{2}$, $s_\gamma \sim 4$, and $\eta_e \sim 2$, one gets in case of $|U_s| = |\dot{R}_s| \ll |v_p|$:

$$kT_s \approx 2 R_{s,7}^{-5/8} \left(\frac{-\dot{M}}{M_\odot/\text{s}} \right)^{1/4} \left(\frac{\widetilde{M}}{M_\odot} \right)^{1/8} [\text{MeV}]. \quad (98)$$

Inserting this in Eq. (66) and using $L_\nu = 2L_{\nu_e}$ yields

$$\begin{aligned} R_{g,7} \approx 1.13 R_{s,7}^{9/16} (kT_{\nu_e,4})^{-1/2} \left(\frac{L_{\nu,52}(R_g)}{\langle \mu_\nu \rangle_g} \right)^{-1/4} \\ \times \left(\frac{-\dot{M}}{M_\odot/\text{s}} \right)^{3/8} \left(\frac{\widetilde{M}}{M_\odot} \right)^{3/16}, \quad (99) \end{aligned}$$

where the neutrino luminosity at the gain radius, $L_\nu(R_g)$, is given by Eq. (76).

Instead of the exact expression of Eq. (97) an approximation for ΔM_g is sometimes preferable. Performing the

integration of Eq. (96) with the approximate density profile of Eq. (63), one finds

$$\Delta M_g \approx 4\pi \rho_s R_s^3 \ln\left(\frac{R_s}{R_g}\right) \propto \frac{-\dot{M}}{\widetilde{M}^{1/2}} R_s^{3/2} \ln\left(\frac{R_s}{R_g}\right). \quad (100)$$

Here ρ_s was written in terms of R_s by making use of $\rho_s = \beta \rho_p$ and Eq. (44). Moreover, from Eq. (99) one can deduce that $R_s/R_g \propto R_s^{7/16}$ for $|U_s| \ll |v_p|$. An increase of the shock radius therefore means that ΔM_g will also grow.

The rate at which the mass in the gain region changes in time due to a shift of the upper and lower boundaries of this region but also due to a variation of the density of the stellar medium, is determined as the total time derivative of Eq. (96):

$$\frac{d}{dt}(\Delta M_g) = 4\pi R_s^2 \rho_s \dot{R}_s - 4\pi R_g^2 \rho_g \dot{R}_g + \int_{R_g}^{R_s} dr 4\pi r^2 \frac{\partial \rho}{\partial t}, \quad (101)$$

where $\dot{R}_s \equiv dR_s/dt = U_s$ is the shock velocity and $\dot{R}_g \equiv dR_g/dt$ the velocity of the gain radius. When the integration in Eq. (101) is carried out to a radius infinitesimally smaller than R_s with the help of Eq. (2), one obtains

$$\begin{aligned} \frac{d}{dt}(\Delta M_g) &= 4\pi R_s^2 \rho_s (\dot{R}_s - v_s) - 4\pi R_g^2 \rho_g (\dot{R}_g - v_g) \\ &= 4\pi R_s^2 \rho_p \dot{R}_s - 4\pi R_g^2 \rho_g \dot{R}_g - \dot{M} + \dot{M}', \end{aligned} \quad (102)$$

with v_g and v_s being the velocities of the stellar medium at the gain radius and just behind the shock, respectively. The lower expression was derived by using the shock jump condition for the mass flow, Eq. (36), and the definitions $\dot{M} = 4\pi R_s^2 \rho_p v_p$ and $\dot{M}' = 4\pi R_g^2 \rho_g v_g = 4\pi R_g^2 \rho_\nu v_\nu$ as introduced in Sect. 7. Equation (102) shows that the mass in the gain region can change because of inflow and outflow of gas but also due to the motion of the boundaries R_g and R_s . Knowing the initial mass in this layer, ΔM_g^0 , Eq. (102) allows one to calculate the value at later times.

8.2. Energy in the gain region

Since the postshock matter is effectively in hydrostatic equilibrium (see Sect. 5) the kinetic energy is negligible compared to the internal energy and the gravitational potential energy, and the total energy in the gain region is therefore given by

$$\Delta E_g = \int_{R_g}^{R_s} dr 4\pi r^2 \left[\varepsilon(r) - \frac{G\widetilde{M}}{r} \rho(r) \right]. \quad (103)$$

To evaluate the right hand side, one substitutes $\varepsilon = P/(\Gamma - 1)$, which relates the internal energy density ε and the pressure P for an ideal gas, with the adiabatic index Γ being typically between 4/3 and 5/3, depending

on whether relativistic or nonrelativistic particles, respectively, dominate the pressure. In addition making use of hydrostatic equilibrium [Eq. (47)] or, alternatively, applying the virial theorem, one finds

$$\begin{aligned} \Delta E_g &= \frac{4\pi}{3(\Gamma - 1)} (P_s R_s^3 - P_g R_g^3) \\ &\quad - 4\pi G\widetilde{M} \frac{3\Gamma - 4}{3(\Gamma - 1)} \int_{R_g}^{R_s} dr r \rho(r). \end{aligned} \quad (104)$$

The second term is the gravitational potential energy times $(\Gamma - \frac{4}{3})/(\Gamma - 1)$. An exact expression for the integral is obtained when Eq. (59) is used for $\rho(r)$:

$$\begin{aligned} \int_{R_g}^{R_s} dr r \rho(r) &= \frac{c_1^3}{2} (R_s^2 - R_g^2) + \left(3c_1^2 c_2 + \frac{c_2^3}{R_s R_g} \right) (R_s - R_g) \\ &\quad + 3c_1 c_2^2 \ln\left(\frac{R_s}{R_g}\right). \end{aligned} \quad (105)$$

The coefficients c_1 and c_2 were already defined in Sect. 8.1. For the following discussion an approximation of this integral is sufficient. It can be derived by employing the approximate power law profile for the density, Eq. (63):

$$\int_{R_g}^{R_s} dr r \rho(r) \approx \rho_s \frac{R_s^2}{R_g} (R_s - R_g). \quad (106)$$

The rate at which the total energy in the gain region changes with time can be calculated as the time derivative of Eq. (103). With the definition $l \equiv (\varepsilon + P)/\rho - G\widetilde{M}/r$ one finds

$$\begin{aligned} \frac{d}{dt}(\Delta E_g) &= 4\pi R_s^2 \rho_s l_s \dot{R}_s - 4\pi R_g^2 \rho_g l_g \dot{R}_g \\ &\quad - 4\pi R_s^2 P_s \dot{R}_s + 4\pi R_g^2 P_g \dot{R}_g \\ &\quad + \int_{R_g}^{R_s} dr 4\pi r^2 \left(\frac{\partial \varepsilon}{\partial t} - \frac{G\widetilde{M}}{r} \frac{\partial \rho}{\partial t} \right), \end{aligned} \quad (107)$$

where \dot{R}_s and \dot{R}_g have the same meaning as in Eq. (101). The partial derivatives in the integral can be substituted by Eqs. (2) and (4). Making additional use of Eqs. (5) and (6) and of $\frac{1}{2}\rho v^2 \ll \varepsilon$ yields

$$\begin{aligned} \frac{d}{dt}(\Delta E_g) &= 4\pi R_s^2 \rho_s l_s (\dot{R}_s - v_s) - 4\pi R_g^2 \rho_g l_g (\dot{R}_g - v_g) \\ &\quad - 4\pi R_s^2 P_s \dot{R}_s + 4\pi R_g^2 P_g \dot{R}_g + \int_{R_g}^{R_s} dr 4\pi r^2 Q_\nu. \end{aligned} \quad (108)$$

Now employing the continuity equation for the mass flow across the shock, Eq. (36), and replacing the integral for

the energy exchange with neutrinos between R_g and R_s by $\mathcal{H} - \mathcal{C}$ as given in Eqs. (82) and (87), one ends up with

$$\begin{aligned} \frac{d}{dt}(\Delta E_g) &= 4\pi R_s^2 \rho_p l_s (\dot{R}_s - v_p) - 4\pi R_g^2 \rho_g l_g (\dot{R}_g - v_g) \\ &\quad - 4\pi R_s^2 P_s \dot{R}_s + 4\pi R_g^2 P_g \dot{R}_g + \mathcal{H} - \mathcal{C} \\ &= 4\pi R_s^2 \rho_p l_s \dot{R}_s - 4\pi R_g^2 \rho_g l_g \dot{R}_g - 4\pi R_s^2 P_s \dot{R}_s \\ &\quad + 4\pi R_g^2 P_g \dot{R}_g - \dot{M} l_s + \dot{M}' l_g + \mathcal{H} - \mathcal{C}. \end{aligned} \quad (109)$$

The mass accretion rates \dot{M} and \dot{M}' account for the inflow of matter into the gain region through the shock and for the mass that is advected through the gain radius, respectively [see Sect. 7 and discussion after Eq. (102)]. Equation (109) means that the total energy in the gain region changes due to active mass motions, $p dV$ work associated with these mass motions, the movement of the boundaries, and neutrino heating.

Making use of $\varepsilon_s = P_s/(\Gamma-1)$, $\rho_s/\rho_p = \beta$, and Eq. (39), one finds for $l_s = (\varepsilon_s + P_s)/\rho_s - G\widetilde{M}/R_s$:

$$l_s \approx - \left[1 - \frac{\Gamma}{\Gamma-1} \frac{\beta-1}{\beta^2} \left(1 - \frac{U_s}{v_p} \right)^2 \right] \frac{G\widetilde{M}}{R_s}, \quad (110)$$

where Eq. (43) with $\alpha \approx 1/\sqrt{2}$ was employed for $v_p^2 \approx G\widetilde{M}/R_s \approx 1.3 \times 10^{19} R_{s,7}^{-1} (\widetilde{M}/M_\odot)$ erg g⁻¹. Because of hydrostatic equilibrium a simple relation exists between l_g and l_s . With $\varepsilon = P/(\Gamma-1)$ and Eqs. (56) and (59) one obtains

$$l_g = l_s - \frac{3\Gamma-4}{4(\Gamma-1)} \frac{G\widetilde{M}}{R_s} \left(\frac{R_s}{R_g} - 1 \right). \quad (111)$$

Using the more general density-pressure relation $P = K\rho^\gamma$ instead of Eq. (56), and the corresponding hydrostatic density profile of Eq. (62), leads to

$$l_g = l_s - \left(1 - \frac{\Gamma}{\Gamma-1} \frac{\gamma-1}{\gamma} \right) \frac{G\widetilde{M}}{R_s} \left(\frac{R_s}{R_g} - 1 \right). \quad (112)$$

For $\Gamma = \gamma$, this gives $l_g = l_s$.

9. Evolution of shock radius and shock velocity

The model developed in the preceding sections allows one to study the behavior of the supernova shock in response to the processes that play a role in the collapsed stellar core. The physics between the neutron star surface and the shock is constrained by the energy influx from the neutrinosphere on the one hand and the mass accretion into the shock front on the other. Equations (97), (104) [in combination with (105)], and (39) determine the shock radius R_s , the shock velocity U_s , and the postshock pressure P_s . The state of the matter immediately behind the shock and that at the gain radius are related via Eqs. (59)–(61) and (111), the gain radius R_g is given by Eq. (66), and the postshock density ρ_s by Eq. (88).

The mass accretion rate \dot{M} into the shock is a fixed parameter of the problem [in Eq. (46) it is expressed in terms of the constant H which is linked to the structure of the progenitor star]. The rate of mass advection into the neutron star, \dot{M}' , can be calculated from Eq. (93). The radius R_ν and mass M of the neutron star, the neutrinospheric luminosity L_ν , and the spectral temperature of the emitted electron neutrinos T_{ν_e} (assumed to be roughly equal to the temperature T_ν of the stellar gas at the neutrinosphere) are also input parameters. The discussion takes into account the effects of neutrino losses in the cooling region, expressed by Eqs. (74)–(77), and of neutrino heating in the gain region as given by Eqs. (82), (83), and (87).

The time dependence of the considered model requires as initial conditions the values ΔM_g^0 and ΔE_g^0 for the initial mass and energy in the gain region. This couples the subsequent evolution in ΔM_g and ΔE_g , which can be followed with Eqs. (102) and (109), respectively, to the situation that exists right after core bounce. Knowing $\dot{M}'(t)$ allows one to include also the changes of the neutron star mass.

9.1. Shock expansion and acceleration

Combining Eqs. (104) and (106) and using Eq. (60) for P_g in terms of P_s with $K^{3/4} = P_s^{3/4}/\rho_s$, one gets the relation

$$(x - x_0) x^3 \approx \left(\frac{R_g}{R_s} \right)^3 \left[x + \left(\frac{R_s}{R_g} - 1 \right) \right]^4 + 4(3\Gamma - 4) \left(\frac{R_s}{R_g} - 1 \right) x^3. \quad (113)$$

Here x and x_0 were defined as

$$x \equiv P_s \left(\frac{G\widetilde{M}\rho_s}{4R_s} \right)^{-1} \propto \left(1 + U_s \sqrt{\frac{R_s}{G\widetilde{M}}} \right)^2, \quad (114)$$

$$x_0 \equiv 3(\Gamma - 1) \frac{\Delta E_g}{4\pi R_s^3} \left(\frac{G\widetilde{M}\rho_s}{4R_s} \right)^{-1} \propto - \frac{\Delta E_g}{\dot{M} \sqrt{R_s \widetilde{M}}}. \quad (115)$$

The proportionality relations can be verified by using Eqs. (39), (43) (with $\alpha = 1/\sqrt{2}$) and (44).

Equation (113) is the key equation to understand the behavior of the supernova shock under the influence of accretion and neutrino heating. Typically, $\Delta E_g < 0$ during the shock stagnation phase, and therefore $x_0 < 0$. Equation (113) depends on two variables which constrain the conditions at the shock front, namely on $x > 0$ and on $y \equiv R_s/R_g$, for which $y \geq 1$ holds. Fixing the parameters \dot{M} , \dot{M}' and R_s , one can show that a larger value of x and thus a larger U_s requires that x_0 and therefore ΔE_g is bigger (i.e., less negative). Physically, this corresponds to the case where neutrino energy deposition leads to a rising postshock pressure P_s [compare Eq. (114)], which accelerates the shock front. On the other hand, if

$|U_s| \ll |v_p| \approx (G\tilde{M}/R_s)^{1/2}$ the quantity x is essentially constant, and $y \propto R_s^{7/16}$ [cf. Eq. (99)] is the variable which reacts to changes of x_0 . The corresponding discussion is more transparent when Eq. (113) is rewritten in the following form:

$$[x - x_0 + 4(3\Gamma - 4)]x^3y^3 \approx (x + y - 1)^4 + 4(3\Gamma - 4)x^3y^4. \quad (116)$$

For $x_0 < 0$ this equation has a solution \hat{y} which shrinks, if ΔE_g and thus x_0 is larger (i.e., less negative). Therefore the radius R_s of the shock, which is compatible with the assumptions, is smaller. Inversely, if ΔE_g and x_0 are lower (more negative), R_s will be larger. This behavior can be explained by the observation that ΔE_g decreases when matter with negative specific energy is accumulated in the gain region. Such an accumulation of mass will cause a growth of the shock radius. It should be noted that a solution $\hat{y} \geq 1$ of Eq. (116) only exists in case of $x_0 \leq 0$.

From the discussion above follows that for given \dot{M} and \dot{M}' , a necessary condition for shock acceleration, i.e., for $dU_s/dt > 0$, is

$$\frac{d}{dt}(\Delta E_g) > 0. \quad (117)$$

This, however, is not a sufficient criterion for an outward motion of the shock, because $d(\Delta E_g)/dt > 0$ can also imply a shrinkage of R_s if more matter (with negative total energy) is lost from the gain region by advection through the gain radius than is resupplied by gas falling into the shock. Equation (100) shows that a growth of the mass ΔM_g in the gain region will cause an increase of R_s , too. Therefore $dR_s/dt \geq 0$ can be ensured if

$$\frac{d}{dt}(\Delta M_g) \geq 0. \quad (118)$$

In combination with Eq. (117) this condition is sufficient to guarantee that R_s and U_s grow at the same time. Applied to a stalled shock, in which case $U_s = 0$, Eq. (117) together with Eq. (118) can therefore be considered as ‘‘shock revival criterion’’, which states that for an expansion and acceleration of the shock front to occur, the energy in the gain region should increase and simultaneously the mass in the gain region should not decrease.

9.2. Shock revival criterion

If the conditions between neutrinosphere and shock vary slowly with time, $\dot{R}_g \approx 0$ is a good assumption. Since $v_p \neq 0$, Eq. (109) can then be written in the form

$$\frac{d}{dt}(\Delta E_g) \approx -\dot{M}l_s + \dot{M}\left(l_s - \frac{P_s}{\rho_p}\right)\frac{\dot{R}_s}{v_p} + \dot{M}'l_g + \mathcal{H} - \mathcal{C}. \quad (119)$$

Replacing l_s in the bracket on the right hand side of Eq. (119) by Eq. (110) and using Eq. (39) for P_s/ρ_p , one

derives in case of $|U_s| \ll |v_p|$ the expression

$$\begin{aligned} \frac{d}{dt}(\Delta E_g) \approx & -\dot{M}l_s - \dot{M}\left(2 - \frac{1}{\beta} - \frac{\beta-1}{\beta^2} \frac{\Gamma}{\Gamma-1}\right)v_p\dot{R}_s \\ & + \dot{M}'l_g + \mathcal{H} - \mathcal{C}. \end{aligned} \quad (120)$$

This equation is correct to first order in $|\dot{R}_s/v_p| \ll 1$. From the discussion in Sect. 8.2 follows that for an outward acceleration of a stalled shock ($\dot{R}_s = U_s = 0$), a necessary condition is [see Eq. (117)]:

$$\frac{d}{dt}(\Delta E_g) = -\dot{M}l_s + \dot{M}'l_g + \mathcal{H} - \mathcal{C} > 0. \quad (121)$$

Note that neutrino heating (\mathcal{H}) and cooling (\mathcal{C}) in the gain region as well as the mass accretion rate \dot{M} through the shock have a direct influence. But also neutrino losses *below* R_g have an effect by determining \dot{M}' , and a more indirect one by causing additional energy deposition in the gain region, where the neutrino energy extracted from the cooling layer is partly reabsorbed.

The terms proportional to $\dot{M} = 4\pi r^2 \rho_p v_p$ account for the so-called ram pressure of the infalling matter, which is proportional to $\rho_p v_p^2$ and damps shock expansion, because the accretion of matter through the shock yields a negative contribution to the right hand sides of Eqs. (119)–(121). A comparison of Eqs. (120) and (121) shows that the onset of shock expansion enhances this and therefore Eq. (121) gives a minimum requirement.

Instead of just an outward acceleration of the shock, a positive postshock velocity, i.e., $v_s > 0$, may be considered as a stronger criterion for the possibility of an explosion. With $\beta = \rho_s/\rho_p$ and Eq. (36) one derives $v_s = \beta^{-1}(v_p - U_s) + U_s$, which means that $v_s > 0$ translates into $U_s > -v_p/(\beta - 1)$. Since $\beta \gg 1$ [Eq. (41)], this condition is fulfilled while $|U_s/v_p| \ll 1$ still holds. Using this more rigorous criterion will therefore affect the details of the discussion, but will not change the picture qualitatively.

$d(\Delta E_g)/dt > 0$ can be achieved by strong neutrino heating (\mathcal{H} large), but can also result if $\dot{M}'l_g > \dot{M}l_s$. For $l_g = l_s$, which is true when $\Gamma = \gamma$ [see Eq. (112)], this is equivalent to $\dot{M}' < \dot{M}$, i.e., when less mass is accreted through the shock than is lost from the gain region into the neutron star [note that $l_s < 0$; Eq. (110)]. As a consequence, however, the mass between R_g and R_s and therefore the shock radius will decrease, in conflict with the demand for shock expansion (see Sect. 8.2). To make sure the shock expands, also Eq. (118) has to be fulfilled. In case of $U_s = 0$, $\dot{R}_g = 0$, Eq. (102) yields:

$$\frac{d}{dt}(\Delta M_g) = -\dot{M} + \dot{M}' \geq 0 \iff \dot{M} \leq \dot{M}'. \quad (122)$$

Both Eqs. (121) and (122) constrain the parameters for which a revival of the stalled shock can occur.

Steady-state conditions, i.e., $\dot{M}' = \dot{M}$, are a special case for which Eq. (122) becomes obsolete. If in addition

the infalling gas is assumed not to be neutrino-heated, $\mathcal{H} - \mathcal{C} = 0$, the case of stationary adiabatic accretion (Chevalier 1989) can be recovered, where the shock does not move and the shock radius can be determined without following the evolution of mass and energy in the postshock region. Setting the neutrinospheric luminosity equal to zero in the model developed here, however, is not sufficient to exactly reproduce this case, because the model does not only include the neutrino emission from a narrow cooling layer on top of the neutron star, but also the potential reabsorption of the emitted neutrinos outside the gain radius. For large accretion rates $|\dot{M}|$ and large shock radii, the reabsorption probability is not negligible and therefore deviations from the standard accretion scenario occur.

9.3. Conditions for shock revival

The properties of Eq. (121) together with Eq. (122) will now be discussed in more detail. For chosen fixed values of the shock stagnation radius, those combinations of mass accretion rate \dot{M} and neutrinospheric luminosity L_ν will be determined which allow for an outward acceleration of the shock front. For these conditions an explosion driven by neutrino energy deposition may develop.

Assuming $U_s = 0$ the gain radius is given by Eq. (99). For the neutrino luminosity $L_\nu = 2L_{\nu_e}$ will be taken again. The accretion rate \dot{M}' of Eq. (93) can be calculated by using Eqs. (94) and (95). Neutrino effects are evaluated from Eqs. (74)–(77) and Eqs. (83) and (87) with Eq. (88) for the postshock density ρ_s .

Several consistency constraints have to be taken into account to make sure that the assumptions of the analytic model developed in the preceding sections are fulfilled:

- (i) For the gain radius [Eq. (99)] $R_\nu + h \lesssim R_g \leq R_s$ must hold. Here h is the scale height of the exponential neutron star atmosphere, Eq. (51). The left inequality constrains the neutrinospheric luminosity to be $L_\nu \lesssim L_1(\dot{M})$, where the limit L_1 depends on the accretion rate \dot{M} . The right inequality, on the other hand, requires $L_\nu \geq L_2(\dot{M})$.
- (ii) Since the neutrinospheric luminosity L_ν and temperature T_ν are *not* coupled here by the assumption of blackbody emission, Eq. (78) must be satisfied to have $L_{\text{acc}} \geq 0$, i.e., to have a cooling layer outside of the neutrinosphere. This translates into a condition $L_\nu \leq L_3$.
- (iii) The definition of R_g implies that neutrinos transfer energy to the stellar gas for $R_g \leq r \leq R_s$. Therefore Eq. (87) has to fulfill the condition $\mathcal{H} - \mathcal{C} \geq 0$, corresponding to $L_\nu \geq L_4(\dot{M})$. This constraint is similar to the one which follows from the requirement that $R_g \leq R_s$, but somewhat stronger, depending on the value of the ratio between $\langle \mu_\nu \rangle_g$ and $\langle \mu_\nu \rangle^*$.
- (iv) Equation (89) [with \mathcal{H} taken from Eq. (83)] has to be less than about 0.5 to justify the disregard of reab-

sorption of neutrinos emitted from the gain layer. This limits the neutrinospheric luminosity to $L_\nu \lesssim L_5(\dot{M})$.

- (v) The postshock temperature must be $kT_s \gtrsim 1$ MeV because the matter behind the shock is assumed to be completely disintegrated into free nucleons, and α particles therefore do not exist. For this to hold, the absolute value of the mass accretion rate must exceed some lower limit, $|\dot{M}| \gtrsim |\dot{M}_1|$, where \dot{M}_1 depends on the shock radius and the effective mass \widetilde{M} of the remnant.
- (vi) Since self-gravity of the gas between neutrinosphere and shock was neglected, the total mass there must be much smaller than the mass of the neutron star. This requirement leads to an upper limit for the rate of mass accretion: $|\dot{M}| \lesssim |\dot{M}_2|$.

While conditions (i)–(iv) are indispensable for the logical coherence of the model, waiving conditions (v) and (vi) would just reduce the accuracy of the discussion. For example, the framework developed in the previous sections could be generalized such that the (partial) recombination of nucleons to α particles or heavy nuclei at temperatures below about one MeV is taken into account. Item (vi) implies

$$\int_{R_\nu}^{R_s} dr 4\pi r^2 \rho(r) = \int_{R_\nu}^{R_{\text{eos}}} dr 4\pi r^2 \rho(r) + \int_{R_{\text{eos}}}^{R_s} dr 4\pi r^2 \rho(r) \lesssim \int_{R_\nu}^{\infty} dr 4\pi r^2 \rho_1(r) + \int_{R_\nu+h}^{R_s} dr 4\pi r^2 \rho_2(r), \quad (123)$$

where $\rho_1(r) \equiv \rho_\nu \exp[-(r-R_\nu)/h]$ [Eq. (50) with h from Eq. (51)] and $\rho_2(r) \equiv \rho_s (R_s/r)^3$ [Eq. (63)]. A reasonable upper bound for this mass integral is

$$\int_{R_\nu}^{R_s} dr 4\pi r^2 \rho(r) \lesssim \frac{\widetilde{M}}{5}, \quad (124)$$

which limits the allowed accretion rate according to condition (vi).

The sequence of plots in Fig. 3 shows the results of an evaluation of Eqs. (121) and (122) together with the constraints (i)–(vi) for different shock stagnation radii: $R_s = 100, 150, 200, 250$ and 300 km, respectively. The numerical values chosen for the other parameters were: $\widetilde{M} = 1.25 M_\odot$, $R_\nu = 50$ km, $kT_\nu = 4$ MeV, $\beta = 7$, $\Gamma = \gamma = \frac{4}{3}$, $f_g = 1.25$ (corresponding to $\eta_e Y_e \approx 1$ at the neutrinosphere), $q_d = 8.5 \times 10^{18}$ erg g⁻¹, $\langle \mu_\nu \rangle^* = 0.4$, $\langle \mu_\nu \rangle_g = 0.6$, and $\langle \mu_\nu \rangle = 0.7$.

The roots of $d(\Delta E_g)/dt$ and $d(\Delta M_g)/dt$ are represented by the lines labeled with O_E and O_M , respectively. These lines separate regions in the $|\dot{M}|$ - L_ν plane, within which the collapsed stellar core reacts differently to the mass inflow through the shock and to the irradiation by

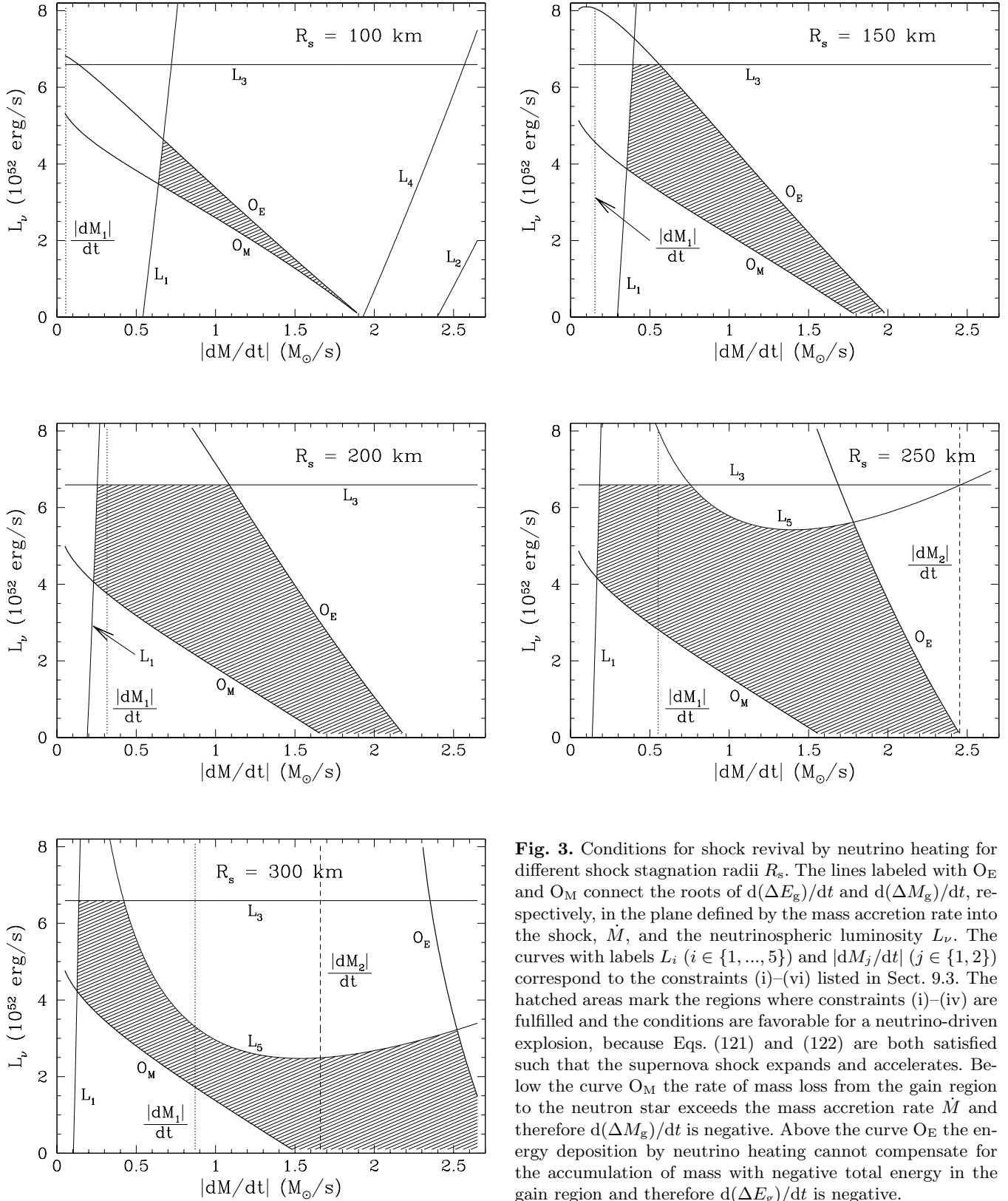


Fig. 3. Conditions for shock revival by neutrino heating for different shock stagnation radii R_s . The lines labeled with O_E and O_M connect the roots of $d(\Delta E_g)/dt$ and $d(\Delta M_g)/dt$, respectively, in the plane defined by the mass accretion rate into the shock, \dot{M} , and the neutrinospheric luminosity L_ν . The curves with labels L_i ($i \in \{1, \dots, 5\}$) and $|dM_j/dt|$ ($j \in \{1, 2\}$) correspond to the constraints (i)–(vi) listed in Sect. 9.3. The hatched areas mark the regions where constraints (i)–(iv) are fulfilled and the conditions are favorable for a neutrino-driven explosion, because Eqs. (121) and (122) are both satisfied such that the supernova shock expands and accelerates. Below the curve O_M the rate of mass loss from the gain region to the neutron star exceeds the mass accretion rate \dot{M} and therefore $d(\Delta M_g)/dt$ is negative. Above the curve O_E the energy deposition by neutrino heating cannot compensate for the accumulation of mass with negative total energy in the gain region and therefore $d(\Delta E_g)/dt$ is negative.

neutrinos emitted from the neutrinosphere. In this respect the plots of Fig. 3 can be considered as “phase diagrams” for the post-bounce evolution of the supernova. Within the hatched areas both Eqs. (121) and (122) and the constraints (i)–(iv) are fulfilled simultaneously. Left of the vertical dotted line, which corresponds to constraint (v), α particles in the postshock medium would have to be taken into account, and the analysis performed here is not very accurate. The vertical dashed line marks the boundary right of which Eq. (124) and thus constraint (vi) are violated.

The hatched area in each plot includes those conditions for which the shock expands and is accelerated. The plots of Fig. 3 therefore show that for given L_ν there is not only an upper limit of $|\dot{M}|$ for which shock expansion and acceleration are possible, but also a lower limit. On the other hand fixing the value of the mass accretion rate, favorable conditions for an explosion are realized only when the neutrinospheric luminosity is between a maximum and a minimum value.

Below the O_M line neutrino cooling above the neutrinosphere is very efficient and the neutron star swallows matter faster than gas is resupplied by accretion through the shock. Therefore $d(\Delta M_g)/dt$ is negative and the shock retreats. Above the O_E line neutrino heating [represented by the term $\mathcal{H} - \mathcal{C}$ in Eq. (121)] cannot compete with the accumulation of matter with negative total energy in the gain layer. This accumulation proceeds very quickly, because the large value of the neutrinospheric luminosity L_ν strongly reduces the neutrino losses from the cooling region and thus the rate of mass advection into the neutron star. Although R_g can grow for such conditions, this does not lead to an explosion, because the postshock matter remains gravitationally bound ($\Delta E_g < 0$).

The distance between the lines denoted by O_M and O_E depends on the $\mathcal{H} - \mathcal{C}$ term in Eq. (121). Therefore it increases with a larger shock radius and thus growing gain region. This can be seen in the plots of Fig. 3 where shock expansion and acceleration are “easier” for a larger value of R_s , i.e., the same core luminosity can ensure favorable conditions already for a higher value of $|\dot{M}|$. When $|\dot{M}|$ drops below a certain critical value, however, continued shock expansion can be supported only by an increasing core luminosity, otherwise advection through the gain radius extracts mass from the neutrino-heating region and the shock expansion breaks down.

9.4. Convective energy transport

The simplified analytic model described in this paper can certainly not account for the detailed effects associated with convective overturn in the neutrino-heated layer between gain radius and shock. This overturn is an intrinsically multi-dimensional phenomenon where low-entropy downflows and hot, rising bubbles of neutrino-heated gas coexist in the same region of the star. Therefore the mix-

ing achieved by the gas motions is not complete. Nevertheless, some consequences and fundamental effects associated with the existence of convective energy transport in the gain region can be figured out.

Using the developed framework of equations with $P = K\rho^\gamma$, $\gamma = \Gamma = \text{const}$, and $K = \text{const}$ for the equation of state in the gain region — which is the default setting for the analyses in Sect. 9 —, one effectively assumes that convection is very efficient in carrying energy from the gain radius, close to which neutrino heating is strongest, to directly behind the shock. This is visible from Eq. (112), according to which the total specific energy at R_g and R_s is the same in this case. Choosing instead $\gamma > \Gamma$ yields $l_g > l_s$, a result which is more characteristic of the situation without convection. Here the energy deposition by neutrinos establishes negative gradients of the entropy and specific energy between gain radius and shock.

Repeating the derivations of Sects. 5–9 with $\gamma > \frac{4}{3}$, reveals, on the one hand, that the gain radius R_g is smaller and therefore the net heating in the gain region, $\mathcal{H} - \mathcal{C}$, is larger compared to the “standard” case of $\gamma = \frac{4}{3}$ (because the hydrostatic density and temperature profiles are flatter behind the shock). On the other hand, however, the absence of energy transport from the gain radius to the shock has a severe disadvantage: The gas which is advected inward through R_g , carries away all the energy absorbed from neutrinos before. This reduces the net effect of neutrino heating and is harmful for the shock expansion and acceleration as can be concluded from Eq. (121), where the term $\dot{M}'l_g$ yields a smaller positive or even a negative contribution when $\dot{M}' < 0$ and l_g is negative or positive, respectively.

These arguments are confirmed by an inspection of a spherically symmetric simulation for the collapse and post-bounce evolution of a $15 M_\odot$ progenitor star published recently by Rampp & Janka (2000). After an expansion to more than 350 km, the shock in this model finally recedes to a much smaller radius and fails to produce an explosion. The shock recession is caused (or accompanied) by a rapid decrease of the mass in the gain region, because more matter is flowing through the gain radius than is resupplied by accretion through the shock. In the hydrodynamical simulation one finds that ΔE_g also decreases during this phase, an effect which cannot occur if $l_g = l_s < 0$ [compare Eq. (121)].

This discussion emphasizes the importance of convective energy transport between the gain radius and the shock. Postshock convection reduces the mass loss as well as the energy loss from the gain region, which are associated with the continuous inward advection of neutrino-heated gas during the phase of shock revival. Also an increase of the core luminosity can diminish the accretion of gas into the neutron star by suppressing the net neutrino emission from the cooling layer. Both effects have been demonstrated in numerical simulations to be helpful for an explosion.

10. Summary and conclusions

In this paper an analytic approach was presented which allows one to discuss the conditions for the revival of a stalled supernova shock by neutrino heating. The treatment is time-dependent and can reproduce the stationary limits of accretion by the neutron star as well as mass loss in a neutrino-driven wind. Different from the standard procedure for estimating the steady-state position of an accretion shock, the neutrinospheric temperature is not derived from the requirement that the neutron star must be able to accrete gas at a given rate. Instead, the rate at which matter can be integrated into the forming neutron star is assumed to be governed by the temperature and luminosity at the neutrinosphere. The latter are determined by the energy transport due to neutrino diffusion from the hot interior to the surface of the newly formed neutron star. This also regulates the gas temperature which is present just above the neutrinosphere: Since the cross sections for neutrino-matter interactions, and thus the opacity of the stellar medium to neutrinos, rise strongly with the mean neutrino energy, an increase (decrease) of this temperature causes a shift of the position of the neutrinosphere to a lower (higher) density and temperature. Therefore the neutrinospheric temperature is typically a rather inert quantity.

The model developed here includes a number of simplifying assumptions. For example, the neutron star is treated as a point mass, i.e., the gravity of the atmosphere above the neutrinosphere is neglected, general relativistic effects are ignored, and the recombination of nucleons to α particles in the postshock matter below a temperature of about 1 MeV is not taken into account. Although the luminosity produced by the accretion of matter is added to the neutrinospheric luminosity of the nascent neutron star, the feedback of the accretion on the neutron star properties and emission is not accounted for. Nevertheless, the model provides interesting insights into the interdependence of effects and processes which determine the post-bounce history of the collapsed stellar core and the evolution of the supernova shock.

In particular, it demonstrates how the mass ΔM_g and the total energy ΔE_g of the gain layer, where neutrinos deposit energy, and the properties of the supernova shock, i.e., its radius R_g and velocity U_s , react in response to different mass infall rates \dot{M} and neutrinospheric luminosities L_ν . Applied to a stalled shock, a shock revival criterion could be derived which formulates the minimum requirements for shock expansion and acceleration as conditions for the development of an explosion. The \dot{M} - L_ν plane can be considered as a phase diagram for the post-bounce evolution of the collapsed stellar core, where basically three regimes have to be discriminated, which are separated by the lines connecting the roots of $d(\Delta M_g)/dt$ and $d(\Delta E_g)/dt$, respectively. For low core luminosities (and a given value of the mass accretion rate), the energy

loss by neutrino emission in the cooling layer below the gain radius is very efficient and the mass advection into the forming neutron star faster than mass can be resupplied by gas infall into the shock. For high core luminosities, the situation is opposite, and gas is accumulated in the gain region, which pushes the shock to larger radii. By itself, this cannot produce an explosion, because the mass in the gain region has negative total energy and is gravitationally bound. At intermediate values of the core neutrino luminosity, however, the energy input by neutrino heating is strong enough to make sure that also $d(\Delta E_g)/dt$ is positive. These are therefore favorable conditions for the neutrino-driven delayed mechanism to work.

When the supernova shock has reached a radius of more than typically ~ 250 km, the gain region is large enough such that the neutrino energy deposition always dominates the influx of negative specific energy associated with the infall of matter through the shock. In this case the efficiency of neutrino energy transfer to the gain region does not pose a constraint on the possibility for an explosion any more. Another effect, however, can still be harmful and prevent further shock expansion: If the neutrinospheric luminosity drops below a critical value, the net energy loss from the cooling region increases to a level where the mass accretion by the neutron star is larger than the infall rate to the shock. As a consequence, gas is lost from the gain region and the shock retreats. It must be suspected that this, and *not* insufficient neutrino heating in the gain region, is the primary reason why spherically symmetric simulations have failed to produce explosions although the shock had expanded to large radii, at least for some period of the post-bounce evolution (see, e.g., Bruenn 1993, Bruenn et al. 1995, Rampp & Janka 2000). An inspection of the hydrodynamical model published by Rampp & Janka (2000) confirms these arguments.

In fact, the decreasing mass infall rate to the shock suggests that the conditions for neutrino-driven explosions become less favorable at “very late” times after core bounce, unless for some reason the *core* neutrino luminosity (not necessarily the total luminosity including the neutrino emission from the accreted gas) rises. Convective energy transport inside the nascent neutron star might produce such an increase of the neutrinospheric luminosity (Burrows 1987, Keil et al. 1996).

The simplified analysis performed in this work, although not able to account for the corresponding effects in detail, nevertheless is able to give a hint on the influence and importance of convective overturn in the neutrino-heated layer. The convective motions transport hot matter and thus energy from the zone of strongest neutrino energy deposition just outside the gain radius to positions closer behind the shock, and allows mainly cold, low entropy material to penetrate inward into the cooling region. This ensures that the energy loss associated with the inward advection of gas through the gain radius is reduced. According to the discussion in this paper this enlarges the

space of conditions in the \dot{M} - L_ν plane where favorable conditions exist for an expansion and acceleration of the supernova shock. Therefore explosions can occur even for cases where spherically symmetric models fail.

Acknowledgements. It is a pleasure to thank M. Rampp for comments on the manuscript, his patience in many discussions, and a comparative evaluation of his spherically symmetric hydrodynamical simulations. The author acknowledges the preparation of Fig. 2 by Mrs. H. Krombach, and help by M. Bartelmann to tame the “ \LaTeX devil”. This work was supported by the SFB-375 “Astroparticle Physics” of the Deutsche Forschungsgemeinschaft.

References

- Bethe H.A., 1990, *Rev. Mod. Phys.* 62, 801
 Bethe H.A., 1993, *ApJ* 412, 192
 Bethe H.A., 1995, *ApJ* 449, 714
 Bethe H.A., 1996a, *ApJ* 469, 737
 Bethe H.A., 1996b, *ApJ* 473, 343
 Bethe H.A., 1996c, *Nucl. Phys. A* 606, 95
 Bethe H.A., 1997, *ApJ* 490, 765
 Bethe H.A., Wilson J.R., 1985, *ApJ* 295, 14
 Bloom J.S., *et al.*, 1999, *Nat* 401, 453
 Bludman S.A., Van Riper K.A., 1978, *ApJ* 224, 631
 Brown G.E., Weingartner J.C., 1994, *ApJ* 436, 843
 Bruenn S.W., 1985, *ApJ Suppl.* 58, 771
 Bruenn S.W., 1986a, *ApJ* 311, L69
 Bruenn S.W., 1986b, *ApJ Suppl.* 62, 331
 Bruenn S.W., 1989a, *ApJ* 340, 955
 Bruenn S.W., 1989b, *ApJ* 341, 385
 Bruenn S.W., 1993, in *Nuclear Physics in the Universe*, eds. Guidry M.W. and Strayer M.R., Institute of Physics Publ., Bristol, p. 31
 Bruenn S.W., Mezzacappa A., Dineva T., 1995, *Phys. Rep.* 256, 69
 Burrows A., 1987, *ApJ* 318, L57
 Burrows A., Goshy J., 1993, *ApJ* 416, L75
 Burrows A., Lattimer J.M., 1986, *ApJ* 307, 178
 Burrows A., Sawyer R.F., 1998, *Phys. Rev. C* 58, 554
 Burrows A., Sawyer R.F., 1999, *Phys. Rev. C* 59, 510
 Burrows A., Hayes J., Fryxell B.A., 1995, *ApJ* 450, 830
 Burrows A., Young T., Pinto P.A., Eastman R., Thompson T., 2000, *ApJ*, in press (astro-ph/9905132)
 Chevalier R.A., 1989, *ApJ* 346, 847
 Colgate S.A., White R.H., 1966, *ApJ* 143, 626
 Colgate S.A., Fryer C., 1995, *Phys. Rep.* 256, 5
 Colgate S.A., Herant M., Benz W., 1993, *Phys. Rep.* 227, 157
 Cooperstein J., Bethe H.A., Brown G.E., 1984, *Nucl. Phys. A* 429, 527
 Fryer C.L., 1999, *ApJ* 522, 413
 Fryer C.L., Benz W., Herant M., 1996, *ApJ* 460, 801
 Galama T.J., *et al.*, 1998, *Nat* 395, 670
 Herant M., Benz W., Hix W.R., Fryer C.L., Colgate S.A., 1994, *ApJ* 435, 339
 Hillebrandt W., 1987, in *High Energy Phenomena Around Collapsed Stars*, ed. F. Pacini, Reidel, Dordrecht, p. 73
 Höflich P., Wheeler J.C., Wang L., 1999, *ApJ* 521, 179
 Iwamoto K., *et al.*, 1998, *Nat* 395, 672
 Janka H.-Th., 1991a, PhD Thesis, TU München, MPA-Report 587
 Janka H.-Th., 1991b, *A&A* 244, 378
 Janka H.-Th., 1992, *A&A* 256, 452
 Janka H.-Th., 1995, *Astroparticle Physics* 3, 377
 Janka H.-Th., Müller E., 1995, *ApJ* 448, L109
 Janka H.-Th., Müller E., 1996, *A&A* 306, 167
 Janka H.-Th., Keil W., Raffelt G., Seckel D., 1996, *Phys. Rev. Lett.* 76, 2621
 Keil W., Janka H.-Th., Müller E., 1996, *ApJ* 473, L111
 Khokhlov A.M., Höflich P.A., Oran E.S., Wheeler J.C., Wang L., Chtchelkanova A.Y.U., 1999, *ApJ* 524, L107
 Lichtenstadt I., Khokhlov A.M., Wheeler J.C., 1999, preprint, submitted to *ApJ*
 Liebendörfer M., Mezzacappa A., Thielemann F.-K., Messer O.E.B., Hix W.R., Bruenn S.W., 2000, preprint (astro-ph/0006418)
 MacFadyen A., Woosley S.E., 1999, *ApJ* 524, 262
 MacFadyen A., Woosley S.E., Heger A., 1999, *ApJ*, in press (astro-ph/9910034)
 Mayle R., Wilson J.R., 1988, *ApJ* 334, 909
 Messer O.E.B., Mezzacappa A., Bruenn S.W., Guidry M.W., 1998, *ApJ* 507, 353
 Mezzacappa A., Calder A.C., Bruenn S.W., Blondin J.M., Guidry M.W., Strayer M.R., Umar A.S., 1998a, *ApJ* 493, 848
 Mezzacappa A., Calder A.C., Bruenn S.W., Blondin J.M., Guidry M.W., Strayer M.R., Umar A.S., 1998b, *ApJ* 495, 911
 Mezzacappa A., Liebendörfer M., Messer O.E.B., Hix W.R., Thielemann F.-K., Bruenn S.W., 2000, *Phys. Rev. Lett.*, subm. (astro-ph/0005366)
 Myra E.S., Bludman S.A., 1989, *ApJ* 340, 384
 Myra E.S., Bludman S.A., Hoffman Y., Lichtenstadt I., Sack N., Van Riper K.A., 1987, *ApJ* 318, 744
 Qian Y.-Z., Woosley S.E., 1996, *ApJ* 471, 331
 Pons J.A., Reddy S., Prakash M., Lattimer J.M., Miralles J.A., 1999, *ApJ* 513, 780
 Raffelt G.G., Seckel D., 1995, *Phys. Rev. D* 52, 1780
 Rampp M., 2000, PhD Thesis, TU München
 Rampp M., Janka H.-Th., 2000, *ApJ* 539, L33
 Reddy S., Prakash M., Lattimer J.M., 1998, *Phys. Rev. D* 58, 013009
 Reddy S., Prakash M., Lattimer J.M., Pons J.A., 1999, *Phys. Rev. C* 59, 2888
 Rybicki G.B., Lightman A.P., 1979, *Radiative Processes in Astrophysics*, John Wiley & Sons, New York
 Shapiro S.L., Teukolsky S.A., 1983, *Black Holes, White Dwarfs, and Neutron Stars*, John Wiley & Sons, New York
 Shige-yama T., 1995, *Publ. Astron. Soc. Japan* 47, 581
 Suzuki H., 1989, *Neutrino Burst from Supernova Explosion and Proto Neutron Star Cooling*, PhD Thesis, Univ. Tokyo
 Takahashi K., El Eid M.F., Hillebrandt W., 1978, *A&A* 67, 185
 Thompson C., 2000, *ApJ* 534, 915
 Wang L., Wheeler J.C., 1998, *ApJ* 504, L87
 Wilson J.R., 1985, in *Numerical Astrophysics*, eds. J.M. Centrella, J.M. LeBlanc, R.L. Bowers, Jones and Bartlett Publ., Boston, p. 422
 Wilson J.R., Mayle R., 1988, *Phys. Rep.* 163, 63
 Wilson J.R., Mayle R., 1993, *Phys. Rep.* 227, 97

- Wilson J.R., Mayle R., Woosley S.E., Weaver T., 1986, Ann. NY Acad. Sci. 470, 267
- Woosley S.E., 1993, A&A Suppl. 97, 205
- Woosley S.E., Weaver T.A., 1994, in *Supernovae*, eds. Bludman S.A., Mochkovitch R., Zinn-Justin J., North-Holland, Amsterdam, p. 63
- Woosley S.E., Eastman R.G., Schmidt B.P., 1999, ApJ 516, 788
- Woosley S.E., Wilson J.R., Mayle R., 1986, ApJ 302, 19
- Yamada S., 2000, Nucl. Phys. A662, 219
- Yamada S., Toki H., 2000, Phys. Rev. C61, 5803
- Yamada S., Janka H.-Th., Suzuki H., 1999, A&A 344, 533